2015-01-01

Design And Analysis Of A Novel Latch System Implementing Fiber-Reinforced Composite Materials

Francisco Guevara
University of Texas at El Paso, fjguevaraarreola@miners.utep.edu

DESIGN AND ANALYSIS OF A NOVEL LATCH SYSTEM IMPLEMENTING FIBER-REINFORCED COMPOSITE MATERIALS

FRANCISCO JAVIER GUEVARA ARREOLA

Department of Mechanical Engineering

APPROVED:

Pavana Prabhakar, Ph.D., Chair

Yirong Lin, Ph.D.

David A. Roberson, Ph.D.

Charles Ambler, Ph.D.
Dean of the Graduate School

To my family

DESIGN AND ANALYSIS OF A NOVEL LATCH SYSTEM IMPLEMENTING FIBER-REINFORCED COMPOSITE MATERIALS

by

FRANCISCO JAVIER GUEVARA ARREOLA

THESIS

Presented to the Faculty of the Graduate School of

The University of Texas at El Paso

in Partial Fulfillment

of the Requirements

for the Degree of

MASTER OF SCIENCE

Department of Mechanical Engineering

THE UNIVERSITY OF TEXAS AT EL PASO

December 2015

Abstract

The use of fiber-reinforced composite materials have increased in the last four decades in high technology applications due to their exceptional mechanical properties and low weight. In the automotive industry carbon fiber have become popular exclusively in luxury cars because of its high cost. However, Carbon-glass hybrid composites offer an effective alternative to designers to implement fiber-reinforced composites into several conventional applications without a considerable price increase maintaining most of their mechanical properties. A door latch system is a complex mechanism that is under high loading conditions during car accidents such as side impacts and rollovers. Therefore, the Department of Transportation in The United States developed a series of tests that every door latch system comply in order to be installed in a vehicle. The implementation of fiber-reinforced composite materials in a door latch system was studied by analyzing the material behavior during the FMVSS No. 206 transverse test using computational efforts and experimental testing.

Firstly, a computational model of the current forkbolt and detent structure was developed. Several efforts were conducted in order to create an effective and time efficient model. Two simplified models were implemented with two different contact interaction approaches. 9 composite materials were studied in forkbolt and 5 in detent including woven carbon fiber, unidirectional carbon fiber, woven carbon-glass fiber hybrid composites and unidirectional carbon-glass fiber hybrid composites. The computational model results showed that woven fiber-reinforced composite materials were stiffer than the unidirectional fiber-reinforced composite materials. For instance, a forkbolt made of woven carbon fibers was 20% stiffer than a forkbolt made of unidirectional fibers symmetrically stacked in 0° and 90° alternating directions.

Furthermore, Hybrid composite materials behaved as expected in forkbolt noticing a decline in the load-displacement slopes while the percentage of glass fiber increased. In the other hand, results showed that a detent made of only glass fiber layers was preferable than a carbon-glass fiber hybrid detent due to the high stresses shown in carbon fiber layers. Ultimately, forkbolt and detent were redesigned according to their functionality and test results. It was observed that the new design was stiffer than the original by showing a steeper load-displacement curve.

Subsequently, an experimental procedure was performed in order to correlate computational model results. Fiber-reinforced composite forkbolt and detent were waterjet cut from a composite laminate manufactured by Vacuum Assisted Resin Transfer Molding (VART) process. Then, samples were tested according to the computational model. Six testing sample combinations of forkbolt and detent were tested including the top three woven iterations forkbolts from the computational model paired with woven and unidirectional glass fiber detents. Test results showed a stiffness drop of 15% when the carbon fiber percentage decreases from 100% to 75%. Also, it was observed that woven glass fiber detent was superior to the unidirectional glass fiber detent by presenting a forkbolt-detent stiffness 38% higher. Moreover, the new design of forkbolt and detent were tested showing a stiffness increment of 29%. Furthermore, it was observed that fiber-reinforced composite forkbolt and detent did not reach the desired load of 5000 N. However, the redesigned forkbolt made of 100% woven carbon fiber and the redesign detent made of 100% woven glass fiber were close to reach that load. The design review based on test results performed (DRBTR) showed that components did not fail where the computational model concluded to be the areas with the highest maximum principal stress. In contrast to the computational model, all samples failed at the contact area between forkbolt and detent.

Table of Contents

List of Tables

List of Figures

1. Introduction

In the United States, there are more than 800 motor vehicles per 1000 people according to the International Road Federation and still most people does not know what is inside of a motor vehicle and how it works. A motor vehicle by definition is a self-propelled machine that its main function is to transport people or cargo. Most motor vehicles nowadays have a very similar design. One important characteristic of their design is that the driver and passengers are positioned inside of a cabin. Therefore, passengers need a way to get into the vehicle cabin and out. Vehicle doors main function is to allow people get in and out of the vehicle. A vehicle door is composed by a very important component called door latch (shown in Figure 1.1). The door Latch system is a mechanism that closes the door when door is shut. Also, the door latch system is what releases the door when the handle is pulled and more importantly the door latch system is what keeps the door closed while the vehicle is in motion. Consequently, the door latch system is very important for people's safety when they are inside of a vehicle.

Door Latch Systems are regulated by the Department of Transportation in The United States. As it was mentioned, the latch system is a safety component in the vehicle. Therefore, all door locks and door retention components in vehicles sold in the United States comply with the Federal Motor Vehicle Safety Standard (FMVSS) No. 206 [1]. This Standard was developed in 1970 in order to protect vehicle passengers by minimizing their ejections through side door openings in car accidents. Crashes such as frontals, side impacts and rollovers may lead to high loading conditions to the vehicle door structure. Consequently, the department of Transportation developed a combination of tests to simulate the loads, in different directions, that are applied to the latch system during crashes. There are two main tests that applied to the regular door latch, longitudinal

and transverse tests. The longitudinal test consists of applying up to 11,000 N in the direction perpendicular to the face of the Latch. In other words, the load is applied to the vehicle driving direction. The door latch system should be in close position and the system must remain in position when load is applied. In the other hand, the transverse test consists of applying up to 9,000 N in the forkbolt opening direction. The door latch system should also be in close position and the system must remain in position when load is applied. Moreover, the longitudinal and transverse tests are also performed in the secondary latch position. The secondary position is when door is closed but not fully closed. For these two tests the load applied is 4,500 N.

Figure 1.1: Door Latch System Location in Vehicle Door

Door latch systems are complex mechanisms that perform several functions. For example: they release door, keeps door closed and lock vehicle by disabling handles. However, its basic design is very simple. A door latch has two fundamental components, a forkbolt and a detent shown in Figure 1.2. The forkbolt is claw-shaped and it encloses the door striker when door is closed. When door handle is pulled to release door, the Forkbolt rotates to liberate the striker. In the other hand, the detent is the mechanism that avoids the forkbolt to rotate when door is closed. So, in

order to open the door, the detent needs to move to allow the forkbolt to rotate and then set the striker free.

Forkbolt and detent nowadays are composed of two parts: a steel core and a thermoplastic elastomer overmold. The core parts are die cut form a steel sheet. Then, they are overmolded as seen in Figure 1.2. Steel has been used as the core material for many years in the interest of gaining good stiffness to the latch. But, it has been noted over the years that using steel cores may cause some complications. A common complication claimed by automobile manufacturers is that cores get corroded due to ambient exposures and poor door seals. So, steel cores need to be plated and treated to avoid corrosion. Nevertheless, plating process is very inconsistent and costumers are still claiming about it. Moreover, release efforts increase drastically due to high sliding friction caused by steel and plating inconsistency. As is was mentioned, in order to release the door, the detent rotates liberating the forkbolt. Therefore, when the detent rotates there is a sliding friction between the forkbolt and detent as shown in Figure 1.2. In the other hand, thermoplastic overmolds are used to reduce sound while latch encloses the striker and detent contacts forkbolt while closing operation.

Fiber-reinforced composites are finding increasing uses during the last four decades in high technology as well as conventional applications. Specifically, fiber and resin systems have been implemented where designers are looking for specific stiffness, high strength, lightweight and corrosion resistance. For Example, Talib et al. [2] analyzed the development of a carbon-glass hybrid composite automotive drive shaft. Also, Zhang et al. [3] studied lightweight load bearing structures made of hybrid composite laminates reinforced with glass and carbon woven fabrics. There is not a known record of the implementation of fiber-reinforced composites to a latch system.

But, due to their exceptional mechanical properties and other advantages, their application can be analyzed.

The most popular fiber-reinforced composites used in the automotive industry are carbon and glass fibers. While fiber glass composites have been increasingly used to replace steel and other metals in automotive industry [4, 5], the implementation of carbon fiber composites remain low. Carbon fiber composites are lighter, stiffer and stronger than glass fiber composites. But, carbon fiber cost is very high. This is the main reason why carbon fiber composites are currently only used in luxury vehicles. However, numerous works have been carried out in the past in order to implement carbon fiber without a considerable price increment of the composite [6, 7, 8, 9]. Carbon-glass hybrid composites offer an effective way of increasing ultimate strain and impact properties while reducing the overall composite cost. Also, it has been studied that incorporating glass fibers layers into a carbon fiber composite increases the overall stiffness and strength of the composite and price will not be increased as if the whole composite would be made of carbon fiber [10]. Studies in glass-carbon composites are mainly focused in the arrangement of the fibers. For instance, Pandya et al. [6] studied carbon and glass woven fabrics under quasi-static loading and concluded that for hybrid composites, placing glass fabric layers in the exterior and carbon fabric layers in the interior gives higher tensile strength and ultimate tensile strain than placing carbon fabric layers in the exterior and glass fabric layers in the interior. By way of contrast, Dong and Davis [11] studied the flexural behavior of glass and carbon hybrid composite. Their results show that placing carbon fiber laminates in the exterior and glass laminates in the interior gives higher flexural strength due to higher compressive and tensile forces developed during bending in the exterior of specimen than in the interior.

In this Paper, The main objective was to explore the feasibility of implementing carbon, glass and carbon-glass hybrid composite materials into a door latch system. Current forkbolt and detent materials were replaced by composite materials and analyzed according to the FMVSS No. 206 transverse test. The analysis consisted of a Finite Element Analysis (FEA) approximation and experimental testing. In addition, a redesign of the two components was performed to complete the design process as shown in Figure 1.3.

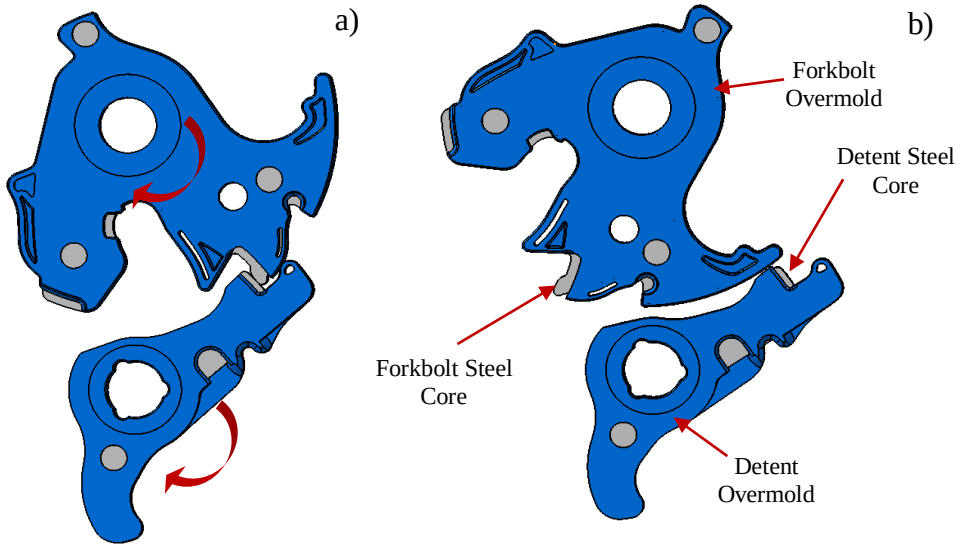

Figure 1.2: Forkbolt and Detent at (a) Close Position (b) Open Position

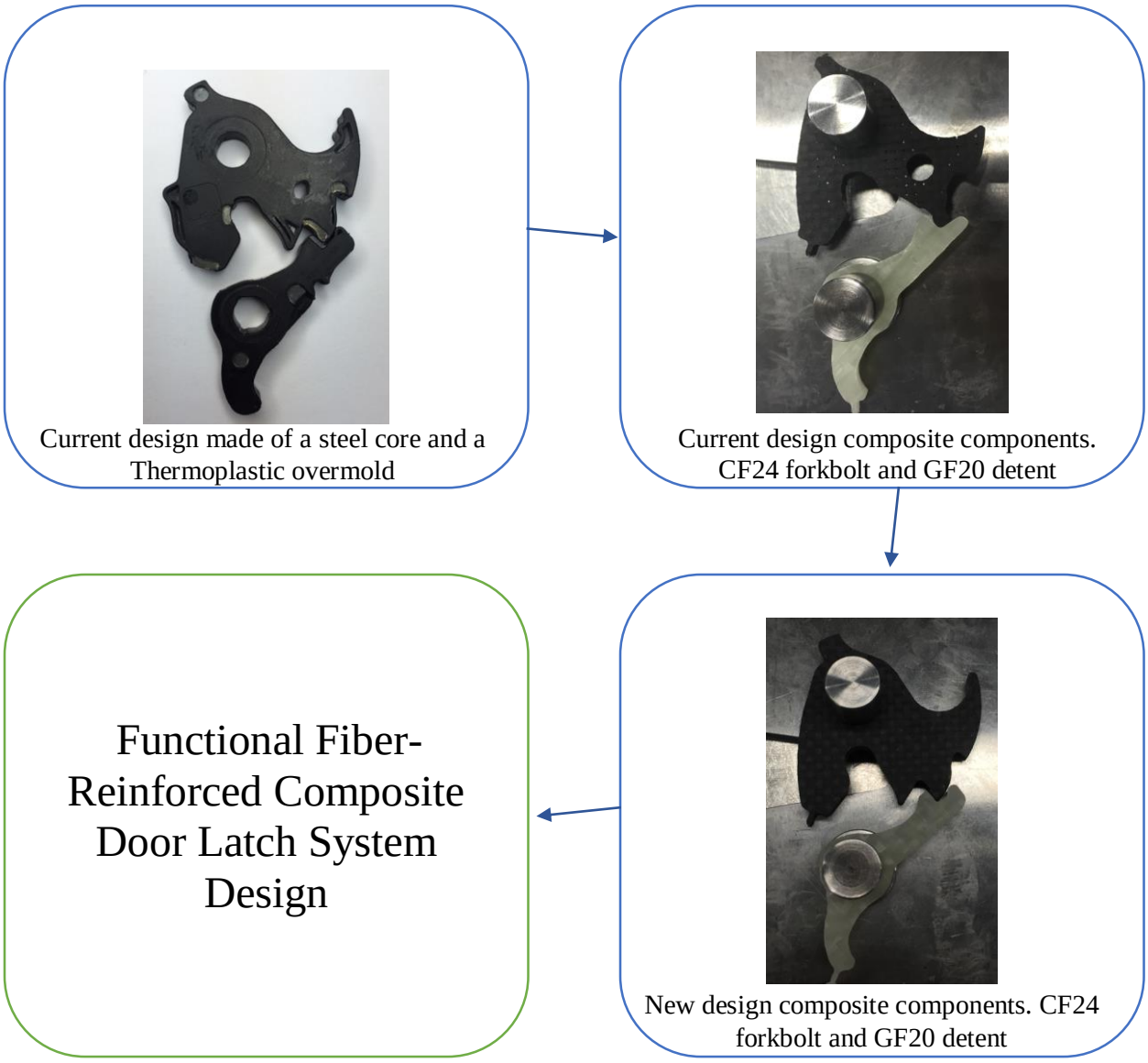

Figure 1.3: Design Process

2. Computational Model

Since the geometry of a door latch system is a very complex mechanism it was a strong need to develop a computational model which was able to approximate testing results. As it was mentioned before a door latch system is built by many components. Therefore, only the forkbolt and detent were analyzed in this study. Firstly, the original design of forkbolt and detent was studied as seen in Appendix A.1. The original design model consisted of six elements: a forkbolt steel core, a forkbolt thermoplastic overmold, a detent steel core, a detent thermoplastic overmold and two steel studs (shown in Figure 2.1). Forkbolt and detent rotate around studs so they needed to be included in the computational model. All CAD models were designed in Unigraphics NX 8.5 commercial software and then imported into ABAQUS commercial software for FEA analysis.

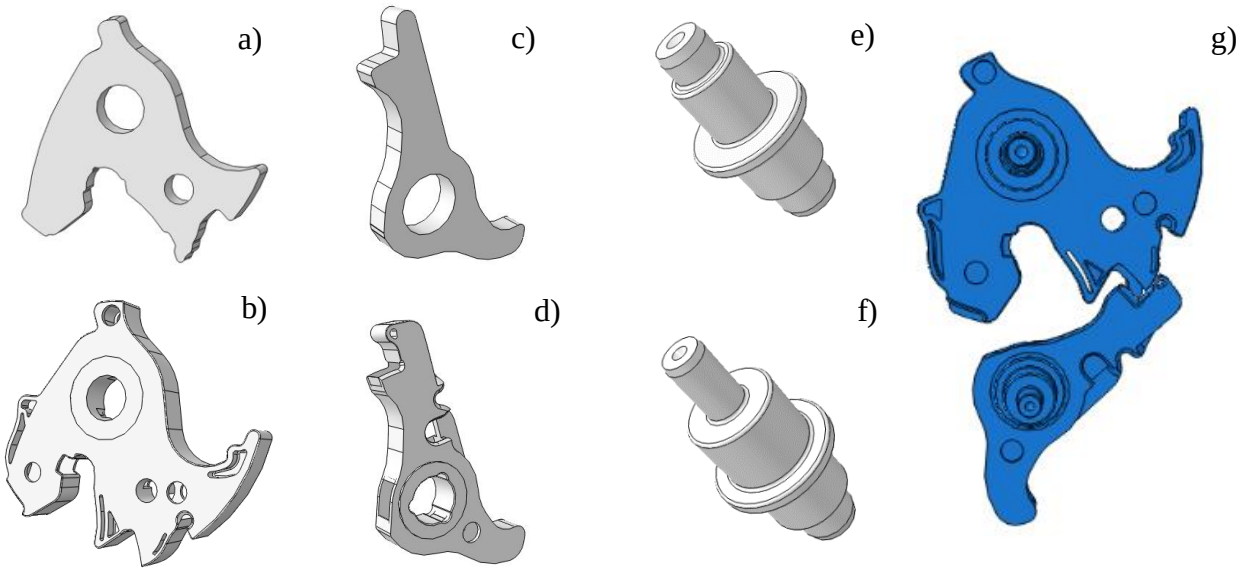

Figure 2.1: Original Design Computational Model Components and assembly: (a) Forkbolt Steel Core, (b) Forkbolt Overmold, (c) Detent Steel Core, (d) detent Overmold, (e) Forkbolt stud, (f) Detent Stud and (g) model assembly

The analysis was developed according to the transverse test in FMVSS No. 206 [1] in which a load of 9,000N is applied to the forkbolt in the opening direction. This test is performed to the whole latch system thus if fewer components are analyzed, a lower load should be applied. Therefore, a Load of 5000N was applied to the same Forkbolt face in this study as explained in Appendix A. Load was applied as displacement and then reaction forces were measured and summed up in the face where displacement was applied. Moreover, stud faces in contact with the other components not analyzed were fixed in the three directions (X, Y, and Z) in order to fix the structure. Furthermore, different contact conditions were studied as seen in Appendix A.1, concluding that there were two approaches to assign contact interaction. One approach was to merge forkbolt, forkbolt overmold and its corresponding stud maintaining their boundaries and material properties. Then, a general contact condition was assigned to the whole model. The second approach was to analyze only Forkbolt subassembly merging forkbolt and forkbolt overmold and fix the forkbolt face in contact with detent. Then, a surface contact condition was assigned to the forkbolt overmold and stud contact faces. The stud face was selected as the master surface and the overmold face as the slave surface. Both approaches gave similar results but the surface contact approach showed preferable stress distribution in forkbolt. As a result of these model parameters, it was possible to analyze forkbolt and detent linear stress. Then, the model was simplified removing the thermoplastic overmolds and replacing the studs by cylinders. The model was simplified for two main reasons. Firstly, because studs geometry is complex and they can be replaced by cylinders. It was noted that this change did not affect computational results. Secondly, the overmolds can be removed from the model since they showed very low stresses when load was applied. The simplified model operate under the same parameters before mentioned.

Consequently, the simplified model consists of four elements: a forkbolt core, a detent core and two cylinders as seen in Figure 2.2.

Figure 2.2: Simplified Computational Model

Subsequently, a modified simplified model was used to study the implementation of composite materials in Forkbolt and detent. Forkbolt and detent thickness was increased by 0.8 mm for two main reasons, Firstly, thickness was increased in order to have a similar thickness than the original design where overmolds enclose core components. Secondly, it was done to accommodate more composite layers into the components increasing component stiffness. Hence, 24 layers for Forkbolt and 20 layers for detent were considered in the analysis with different layer combinations. Carbon fiber and glass fiber layers were examined with the combinations shown in Table 2.1. Forkbolt material iterations were analyzed with the surface contact approach and detent material iterations were analyzed with the general contact approach using CF24 as forkbolt material. Layer thickness was assumed to be the same disregarding the fiber type. Forkbolt and detent were layered and layer material properties were assigned to each layer. Layer material properties are shown in Table 2.2. Figure 2.3 shows a schematic of the cross-section of the layered

Forkbolt to elucidate the terminology used to describe layer combinations with an example of the CF9GF6CF9 combination.

Table 2.1: Layer Combinations

Forkbolt (24 layers)		**Detent (20 layers)**	
Layer combination	Fiber percentage	Layer combination	Fiber percentage
CF24	100%CF	GF20	100%GF
CF9GF6CF9	75%CF 25%GF	CF2GF16CF2	20%CF 80%GF
GF3CF18GF3	75%CF 25%GF	CF3GF14CF3	30%CF 70%GF
CF8GF8CF8	66.6%CF 33.3%GF	CF5GF10CF5	50%CF 50%GF
CF6GF12CF6	50%CF 50%GF		
CF4GF16CF4	33.3%CF 66.6%GF		

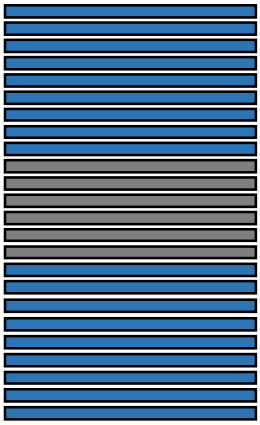

Figure 2.3: Cross-section of a CF9GF6CF9 Laminate

Furthermore, unidirectional fiber layers were considered for the analysis with only one stacking configuration $(0,90,0,90,0,90,0,90,\ 0,90,0,90)_s$ for Forkbolt and $(0,0,0,0,0,0,0,0,0,0)_s$ for detent. By using unidirectional fibers instead of woven fibers is possible to achieve higher fiber volume fraction thus slightly stiffer overall mechanical properties. Unidirectional fibers were

analyzed with the following percentages: 100%CF, 75%CF/25%GF and 66.6%CF/33.3%GF in Forkbolt and 100%GF for detent. It is well known that a woven lamina is thicker than a unidirectional one but the layer thickness remained the same to simplify the model.

2.1 COMPOSITES MECHANICAL PROPERTIES

Two types of fiber-reinforced composites were studied in this paper: composites reinforced by woven fibers and composites reinforced by unidirectional fibers oriented in different directions. For the woven fibers composites, the mechanical properties were obtained from ACP Composites website. In the other hand, for unidirectional fibers composites, the mechanical properties were analyzed with Composite Cylinder Model (CCM) as seen in Appendix A.2. CCM provides the mechanical properties for an individual lamina. CCM was calculated in MATLAB R2015. Table 2.2 shows the Mechanical Properties of composites studied in this paper.

Table 2.2: Mechanical Properties.

	Carbon Fiber	**Carbon/Epoxy**		**S2 Glass Fiber**	**S2 Glass/Epoxy**	
Type	UD	UD Lamina	Woven	UD	UD Lamina	Woven
E11 (GPa)	230	151.7	70	86.9	52.8	27.1
E22 (GPa)	12	10.3	70	10	5.62	27.1
Poisson's ratio	0.3	0.3	0.3	0.3	0.3	0.3

2.2 MODEL MESH

Meshing was performed in ABAQUS having the exact same mesh in all simulations. Three dimensional linear Hexahedron elements were employed in all components. Elements were refined

in principal areas as shown in Figure 2.4. For example, elements that were in contact in the forkbolt-detent contact area were refined by 70% of the global element size. The same refining principle applied for elements near the hook shaped area in forkbolt where structured mesh was assigned in order to obtain superior results. At the end, a total of 124136 elements were used in the general contact approach and 165518 elements for the surface contact approach. Both meshes were verified by the software showing no element warnings.

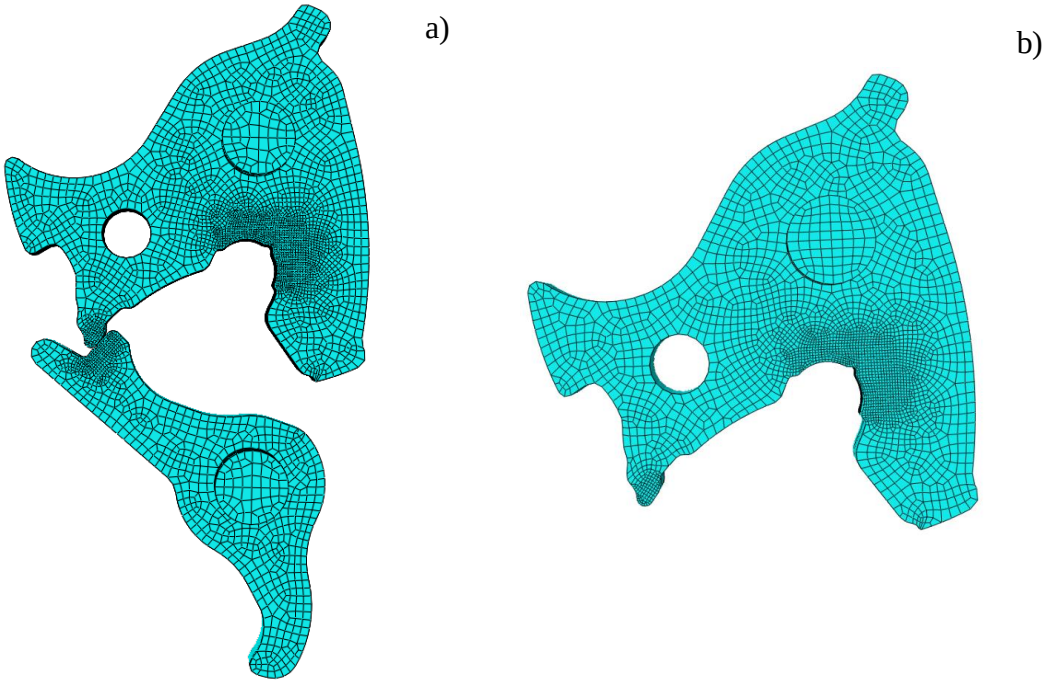

Figure 2.4: Model Mesh of (a) General Contact Approach and (b) Surface Contact Approach

2.3 COMPUTATIONAL MODEL RESULTS

The present computational simulations were utilized to analyze the behavior of fiber reinforced composite materials in a latch system and approximate their performance in a strength test. As mentioned before, two computational models were studied in this paper. One model

analyzes the forkbolt by itself and it was called surface contact approach. The surface contact approach studies the material iterations in forkbolt. Maximum principal stress, stress distribution and load- displacement curve were analyzed in each iteration. In the other hand, forkbolt and detent were analyzed together in a model called general contact approach. It studies the material iterations in detent by maintaining the same material properties in forkbolt. Maximum principal stress, stress distribution and contact pressure were analyzed in each iteration.

Forkbolt material iterations were analyzed by comparing their load-displacement curves and maximum principal stresses. Forkbolt load- displacement curve was determined by summing up the reaction forces of the nodes corresponding to the surface where the displacement was applied and averaging their displacement through the time steps. It was noticed that there were a linear behavior in all load-displacement plots so it was determined to apply the same displacement in all material iterations. A displacement of 0.35mm was chosen from the CF24 iteration where it was observed that it was the displacement needed to exceed 5000N. The CF24 woven material load-displacement plot is shown in Figure 2.5. Then, the load displacement slopes of all material iterations were compared in Figure 2.6. It was observed that woven CF24 was the stiffest material by showing a steeper slope of 15007.29 N/mm than the other materials. Also, it was noticed that for hybrid composite materials the load-displacement slope decreased as the percentage of glass fiber material increased. Therefore, for hybrid woven materials, CF4GF16CF4 with a 66.6% of glass fiber showed the lowest slope of 10866.36 N/mm. In addition, two different stackings with the same hybrid ratio were compared. One stacking located carbon fiber layers in the exterior and glass fiber layers in the interior. The other stacking switched the position of the fibers placing glass fiber layers in the exterior and carbon fiber layers in the interior. Both stackings with 75% of carbon fiber showed very similar load displacement slopes. CF9GF6CF9 was slightly stiffer with

a slope of 13514.81 N/mm than GF3CF18GF3 with a slope of 13505.02 N/mm. Hence the position of the fibers did not affect significantly the material stiffness. Additionally, it was observed that woven composite materials were stiffer than unidirectional materials with the same hybrid ratio. For instance, woven CF8GF8CF8 showed a slope of 12998.08 N/mm and unidirectional CF8GF8CF8 showed a slope of 11656.45N/mm. Moreover, the maximum principal stress of all material iterations was analyzed in forkbolt at an applied displacement of 0.35mm. It is noticed that the forkbolt hook reacts as a cantilever beam when force is applied. As consequence, maximum stresses were found where the hook connects to the rest of the body. It can be observed that stresses increased gradually while the percentage of glass fiber increased. The stress increment was seen in the remaining carbon fiber layers in hybrid composites as seen in Figure 2.9 and Figure 2.10. In other words, the stiffer material in a hybrid composite experienced greater stresses since it was the one giving higher support to the composite. Also, the two hybrid composite stackings with 75% of carbon fiber showed similar stress behavior. However, the stacking with carbon fiber layers in the center showed slightly lower stresses with a maximum of 843.4MPa than the stacking with carbon fiber layers in the exterior with a maximum stress of 855.4MPa. The same behavior in Hybrid composites was presented by Pandya et al. [6] in an experimental study on the in-plane tensile and compressive properties of hybrid composites made using T300 carbon fiber and E-glass fiber. Additionally, unidirectional fiber reinforced composites showed larger stresses than woven fiber reinforced composites as seen in Figure 2.10 (b), (c) and (d). Massive stress concentration was seen in the layers where fibers go in the same direction (fibers in 0°) than the displacement applied. For instance, the unidirectional CF8GF8CF8 showed the highest stresses with a maximum of 1652 MPa. Maximum principal stresses of material iterations were also compared with the steel stresses at steel maximum displacement of 0.065mm as seen in Figure 2.7.

Detent material iterations were analyzed by comparing their maximum principal stress and contact stress behaviors. For this analysis both forkbolt and detent were utilized maintaining the same material properties for forkbolt and iterating the detent material each time. Woven CF24 was chosen to be the material for forkbolt in all general contact simulations because it was the one showing the best stiffness in the surface contact approach. Maximum principal stress was studied for all iterations showing the highest stress concentration in the surroundings of the area in contact with forkbolt. It was observed that detent experienced very low stresses compared to forkbolt results. For instance, the woven GF20 displayed a maximum stress of 71.8MPa which was lower than any other material. Also, CF5GF10CF5 showed the highest stress of 136.8MPa when it was compared to the other material iterations. Additionally, contact stress was studied in order to check the pressure that the forkbolt produced on detent. CF20 showed the lowest maximum contact stress of 558MPa while CF2GF16CF2 showed the highest. Figure 2.8 (b) displays a comparison of the maximum contact stress in all material iterations. For Hybrid iterations it was observed that contact maximum stress decreased while the content of carbon fiber increased. However, an opposite pattern occured in Figure 2.8 (a) where maximum principal stresses were compared. It was observed in Figure 2.11 (a) and (c) and Figure 2.12 (a) and (c) that maximum principal stress increased as the percentage of carbon fiber increased as well.

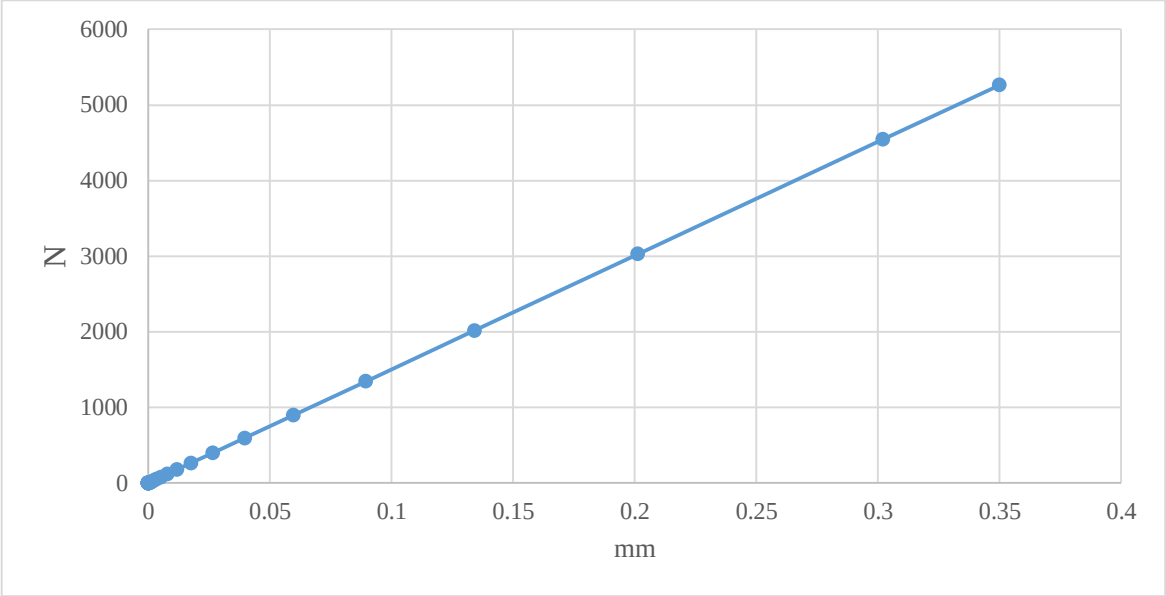

Figure 2.5: CF24 Woven Material Load-displacement Plot

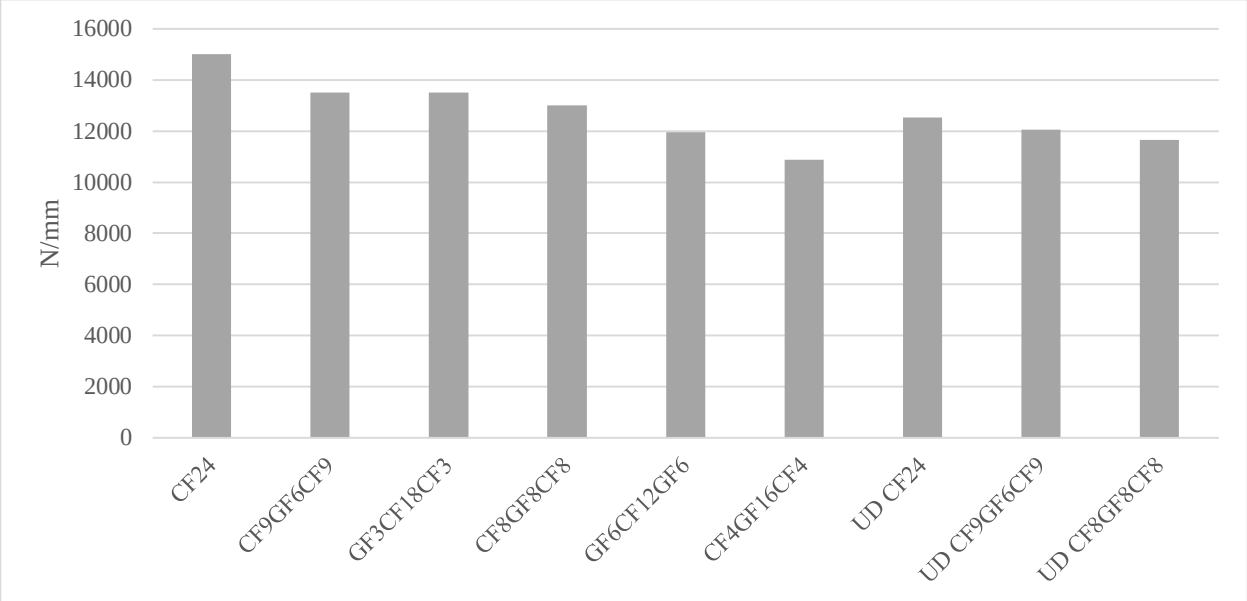

Figure 2.6: Load-displacement Slopes of Forkbolt Material Iterations

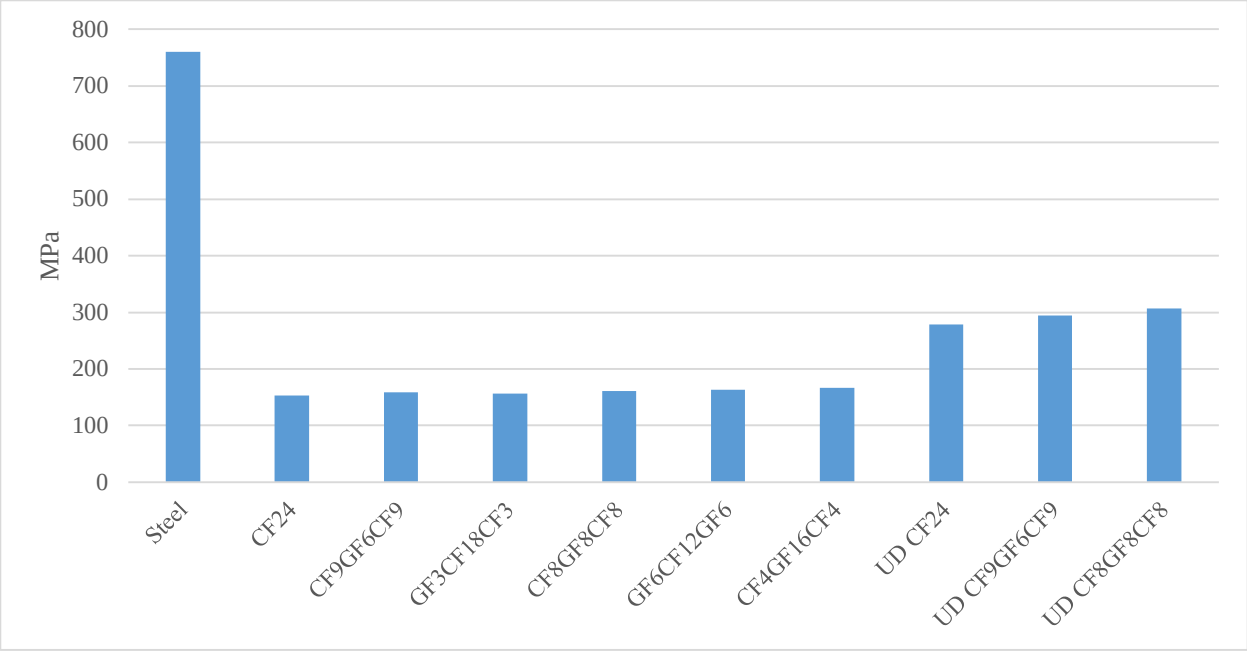

Figure 2.7: Maximum Principal Stresses at an Applied Displacement of 0.065 mm

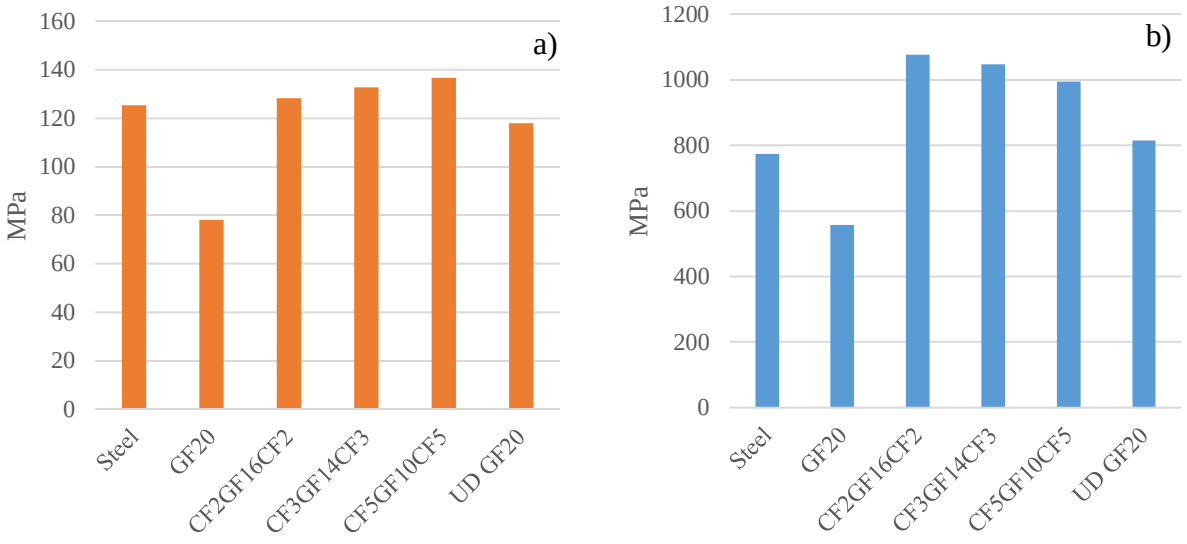

Figure 2.8: Detent Material Iterations (a) Maximum Principal Stress and (b) Contact Pressure at Surface Nodes

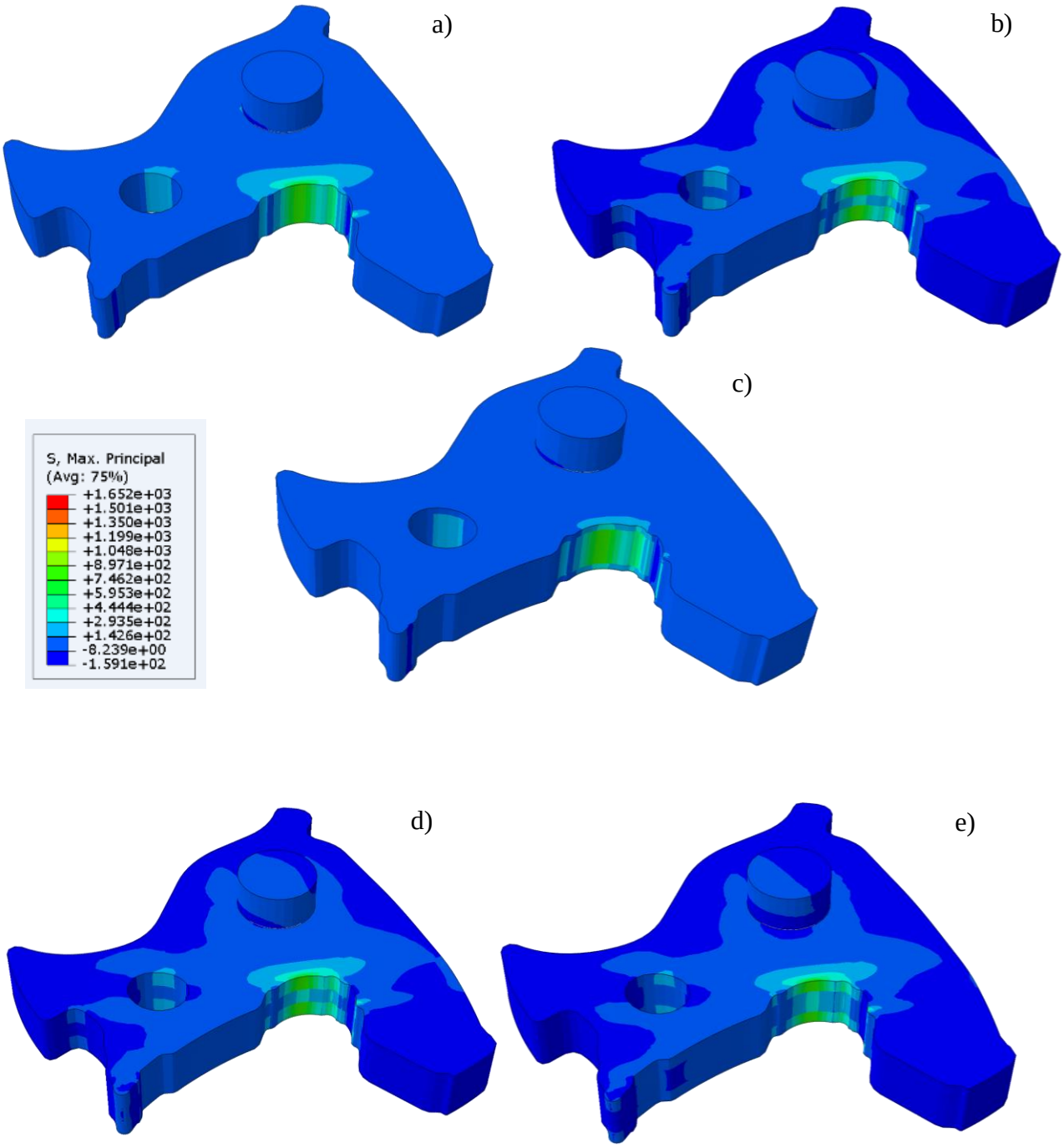

Figure 2.9: Maximum Principal Stress Contours of Woven (a) CF24, (b) CF9GF6CF9, (c) GF3CF18GF3, (d) CF8GF8CF8 and (e) CF6GF12CF6

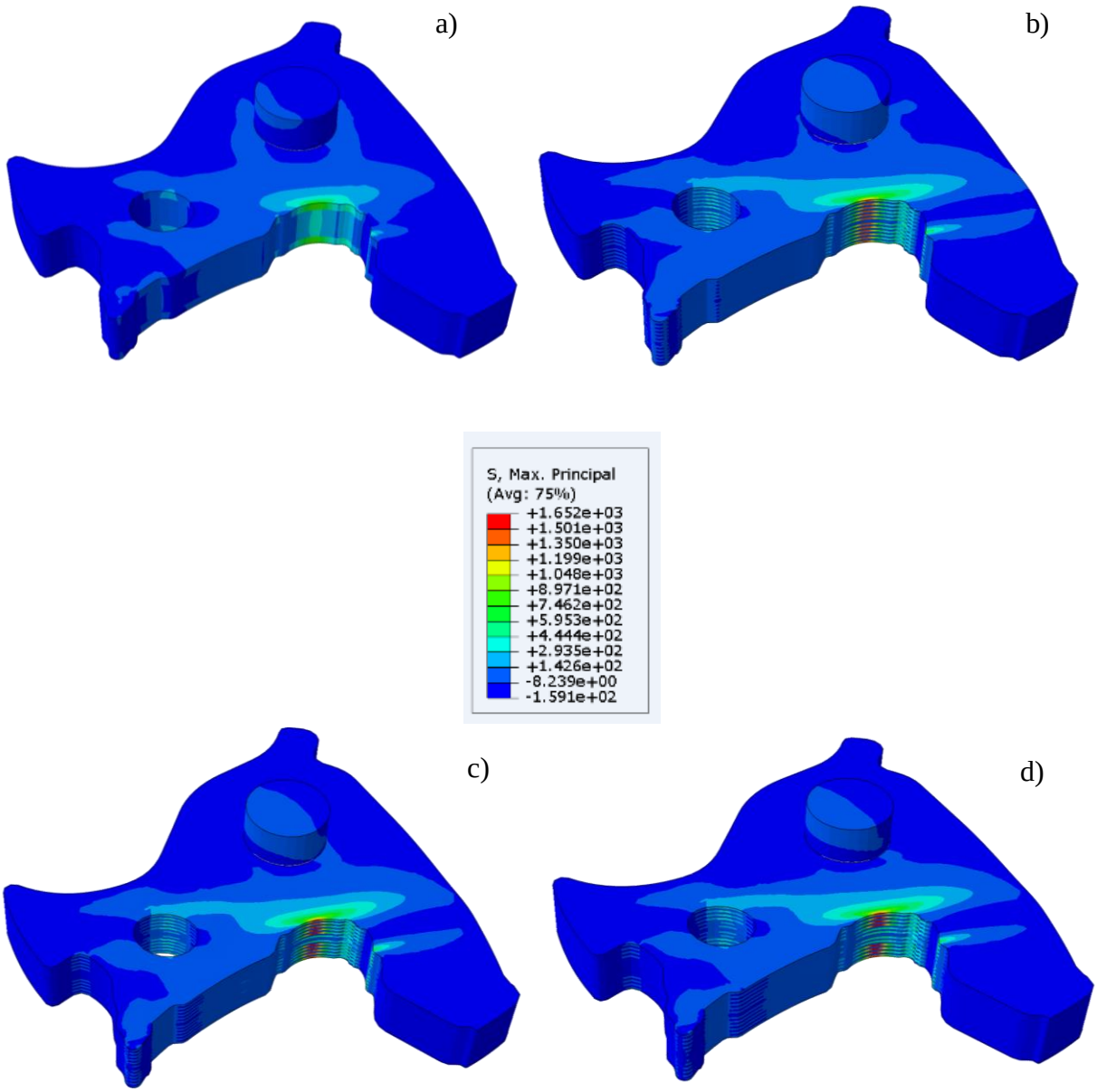

Figure 2.10: Maximum Principal Stress Contours of (a) Woven CF4GF16CF4, (b) Unidirectional CF24, (c) Unidirectional CF9GF6CF9 and (d) Unidirectional CF8GF8CF8

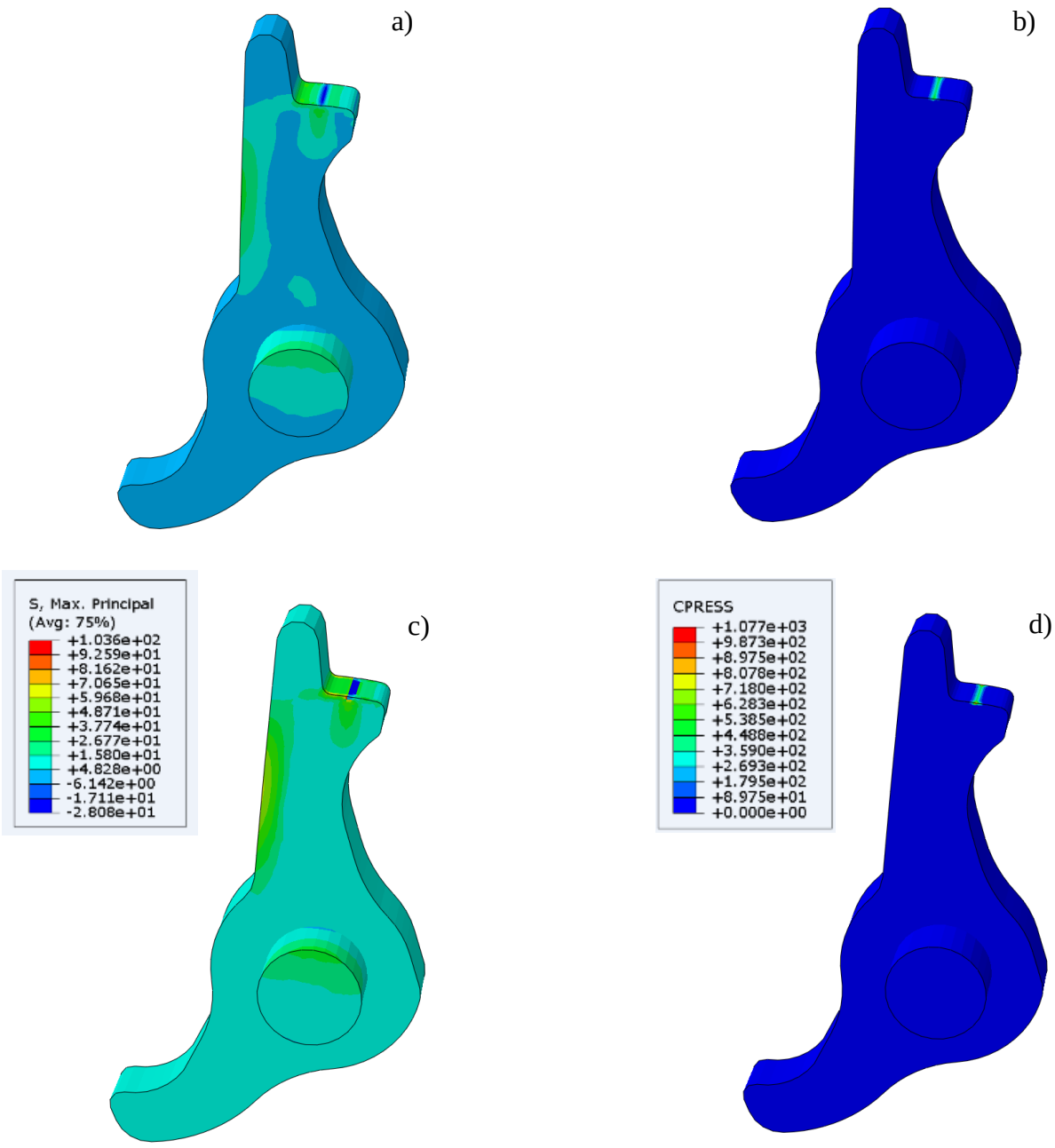

Figure 2.11: Maximum Principal Stress Contours of Woven (a) GF20 and (c) CF2GF16CF2. Contact Pressure contours of (b) GF20 and (d) CF2GF16CF2

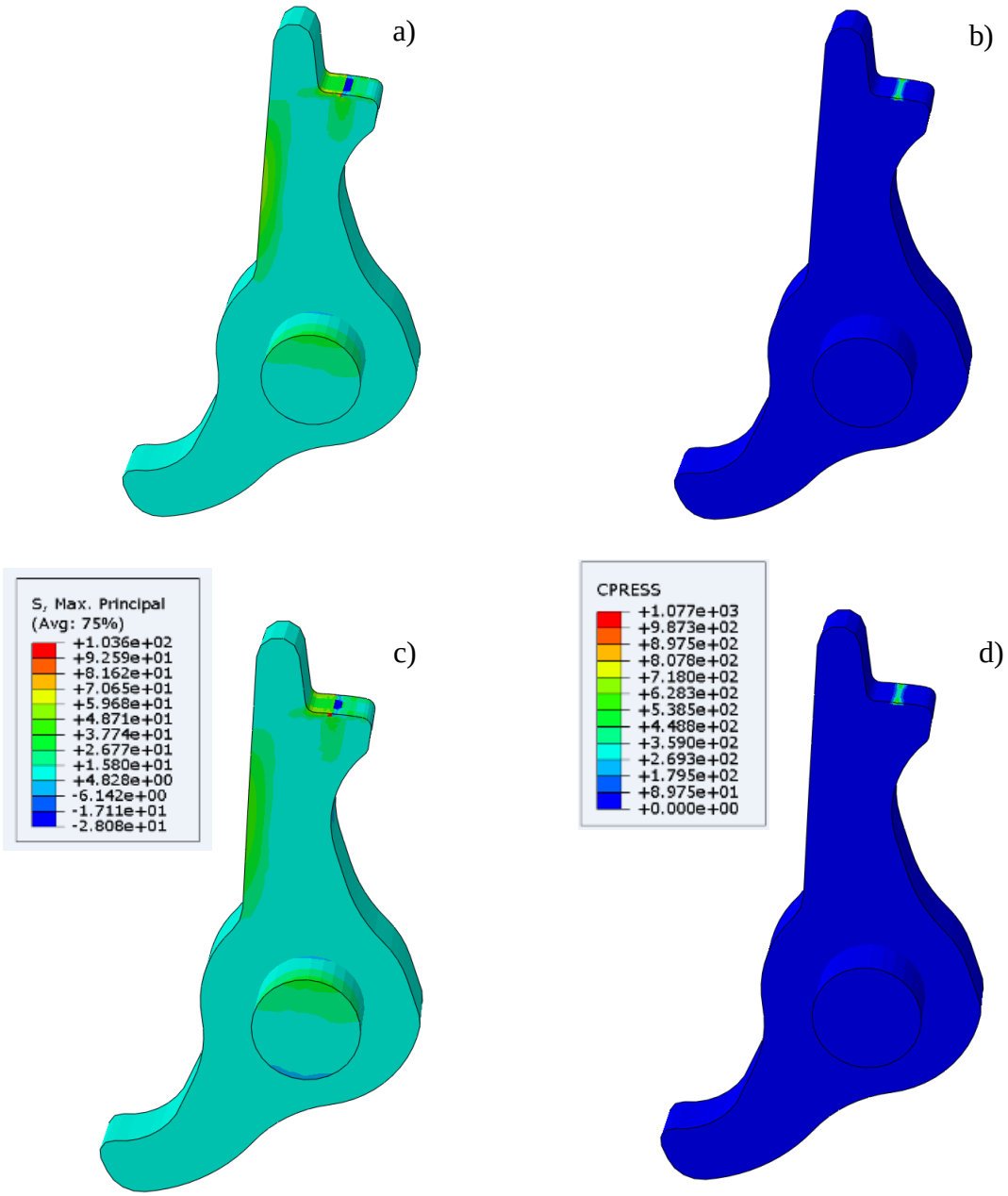

Figure 2.12: Maximum Principal Stress Contours of Woven (a) CF3GF14CF3 and (c) CF5GF10CF5. Contact Pressure contours of (b) CF3GF14CF3 and (d) CF5GF10CF5

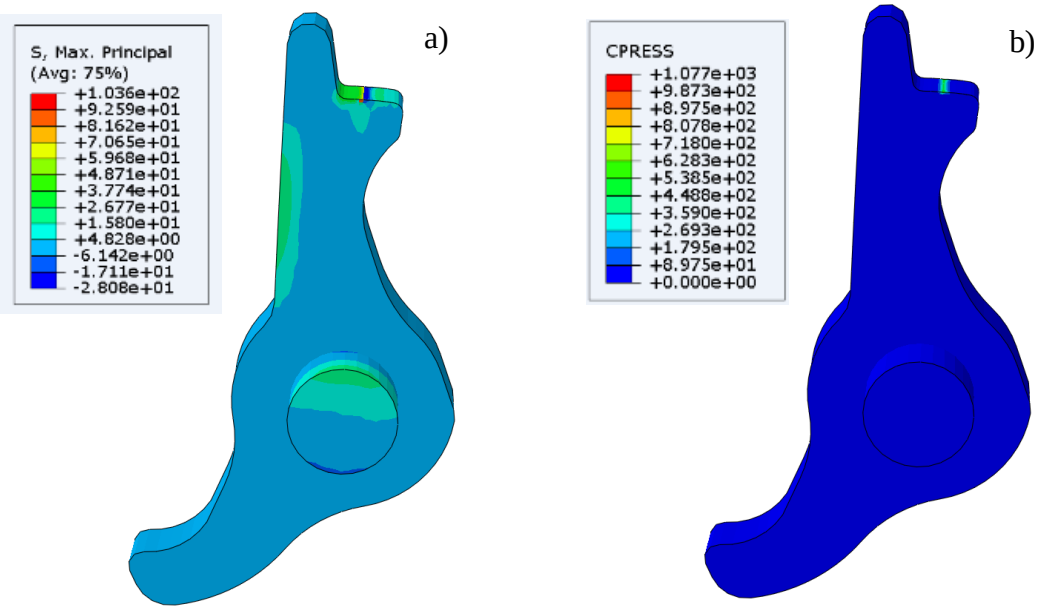

Figure 2.13: Unidirectional GF20 (a) Maximum Principal Stress and (b) Contact Pressure Contours

2.4 Component Redesign based on functionality and computational model results

Forkbolt and detent were redesign based on two main reasons. Firstly, the redesign made forkbolt and detent functional. It was previously mentioned that original forkbolt and detent designs consisted of two parts: a steel core and a thermoplastic overmold. The thermoplastic overmold was removed to simplify the computational model without affecting the results. However, the thermoplastic overmolds have special features on its design that make the design functional on a latch system. So, the same special features were added to the new forkbolt and detent fiber reinforced composite cores. For instance, a tail was added to the forkbolt creating a hook that encloses a bumper when the latch system is in closed position. The bumper restricts the forkbolt to rotate more than the required when it goes to closed position. Secondly, forkbolt and

detent were redesign based on the computational model results previously mentioned. For example, the area that encloses the sticker when door is closed was perfectly rounded eliminating unnecessary features that concentrated stress on that area instead of being nicely distributed. Also, material was added to forkbolt as support on the area in contact with detent. The detent also had some modifications. For instance, a "head" was added on the top to create a second contact with the forkbolt supporting the compression created by forkbolt when it is pulled.

A computational model was done in order to compare results of the new design with the original design. Both computational models consisted of a woven CF24 forkbolt and woven G20 detent analyzed by applying the general contact approach. A displacement of 0.21 mm was applied to forkbolt in both models. As a result, the load displacement curves of both models were compared in Figure 2.14. It was observed that the new design was stiffer than the original one by showing a steeper slope. Also, the new design reached up to 5589.62 N when a displacement of 0.21 was applied. In the other hand, the original design reached 4465.834 N when the same displacement was applied. However, it was noted that since the new design was stiffer, it showed higher maximum principal stresses. Figure 2.15 shows the maximum principal stress distribution in both models. It was noticed that stress was better distributed throughout the components in the new design. Moreover, contact pressure between forkbolt and detent was compared in both designs. Since higher forces were reacted by the redesigned forkbolt, the contact pressure increased from 558.4MPa in the original design to 900 MPa in the new design. Figure 2.16 (e) and (f) shows the contact pressure in both detents.

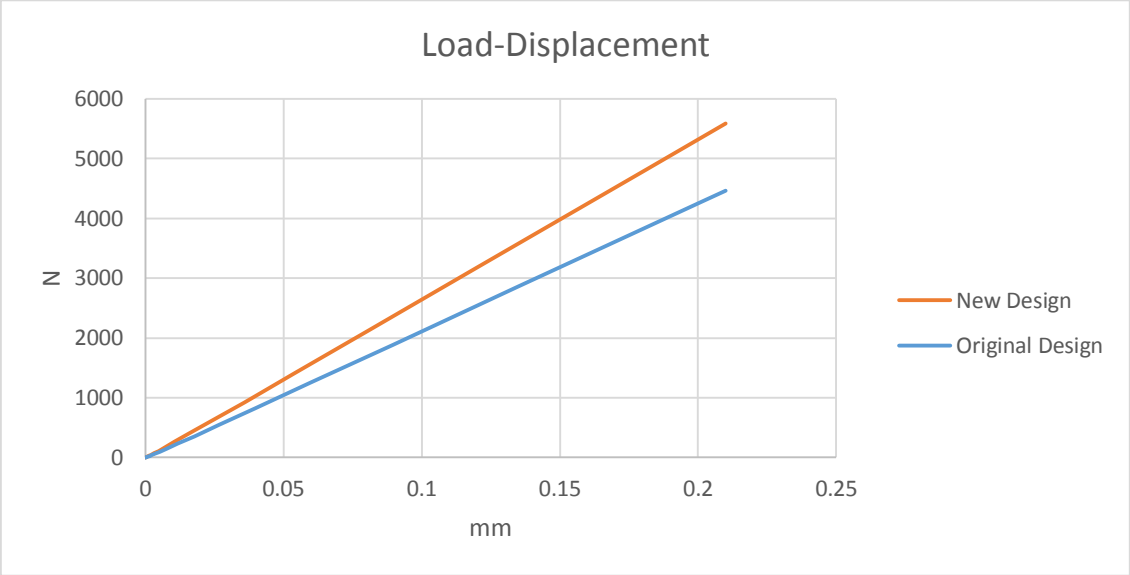

Figure 2.14: Load-displacement Plot Comparing the New Design with the Original Design

a) b)

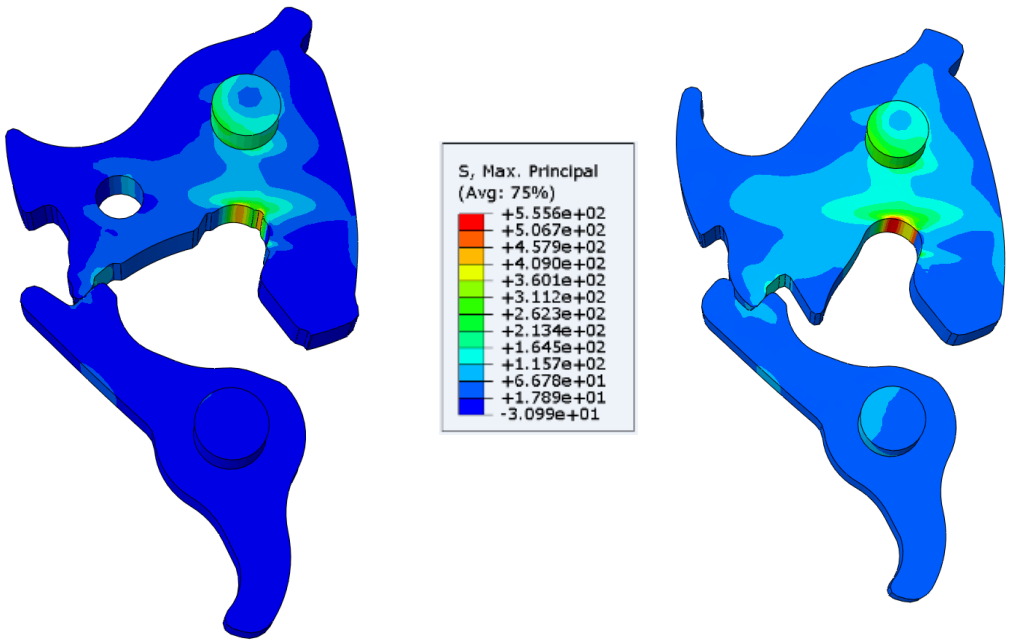

Figure 2.15: Maximum Principal Stress Contours of (a) Original Design and (b) New Design

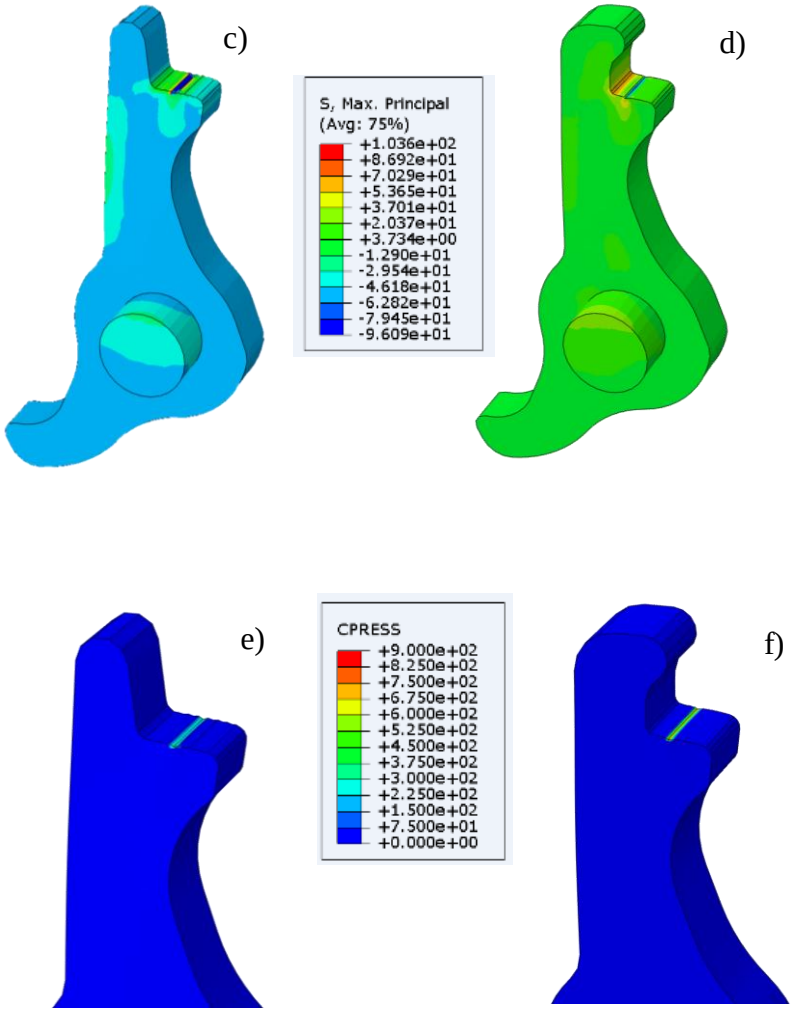

Figure 2.16: Maximum Principal Stress Contours of (c) Original Design and (d) New Design. Contact Pressure Contours of (e) Original Design and (f) New Design

2.5 COMPUTATIONAL MODEL CONCLUDING REMARKS

Three-dimensional linear structural analysis aided to predict the behavior of fiber-reinforced composite materials in a door latch system. It was concluded, that forkbolt and detent of a door latch system can be analyzed by using a simplified computational model with two different contact condition approaches. The surface contact approach can be utilized to analyze forkbolt

independently and the general contact approach is utilized to analyze forkbolt and detent together. Moreover, material properties in forkbolt can be iterated and effectively analyzed by using the surface contact approach instead of the general contact approach due to the preferred stress distribution throughout the part. Also, material iterations can be compared by creating the load-displacement curve of each iteration and comparing their slopes.

In conclusion, woven fiber-reinforced composite materials showed superior results than the unidirectional fiber-reinforced composite materials. For instance, a forkbolt made of woven carbon fibers was 20% stiffer than a forkbolt made of unidirectional fibers symmetrically stacked in 0° and 90° alternating directions. Furthermore, Hybrid composite materials behaved as expected in forkbolt noticing a decline in the load-displacement slopes while the percentage of glass fiber increased. In the other hand, results showed that a detent made of only glass fiber layers was preferable than a carbon fiber-glass fiber hybrid detent due to the high stresses shown in carbon fiber layers. Ultimately, forkbolt and detent were redesigned according to their functionality and test results. The new design showed superior results over the original design. It was noted that the new design was 24% stiffer than the original design.

The present computational model was the first step in the investigation of fiber-reinforced composite materials implementation in a door latch system. The computational model complete framework flow is shown in Figure 2.17. Further experimental testing must be performed to validate the computational model result.

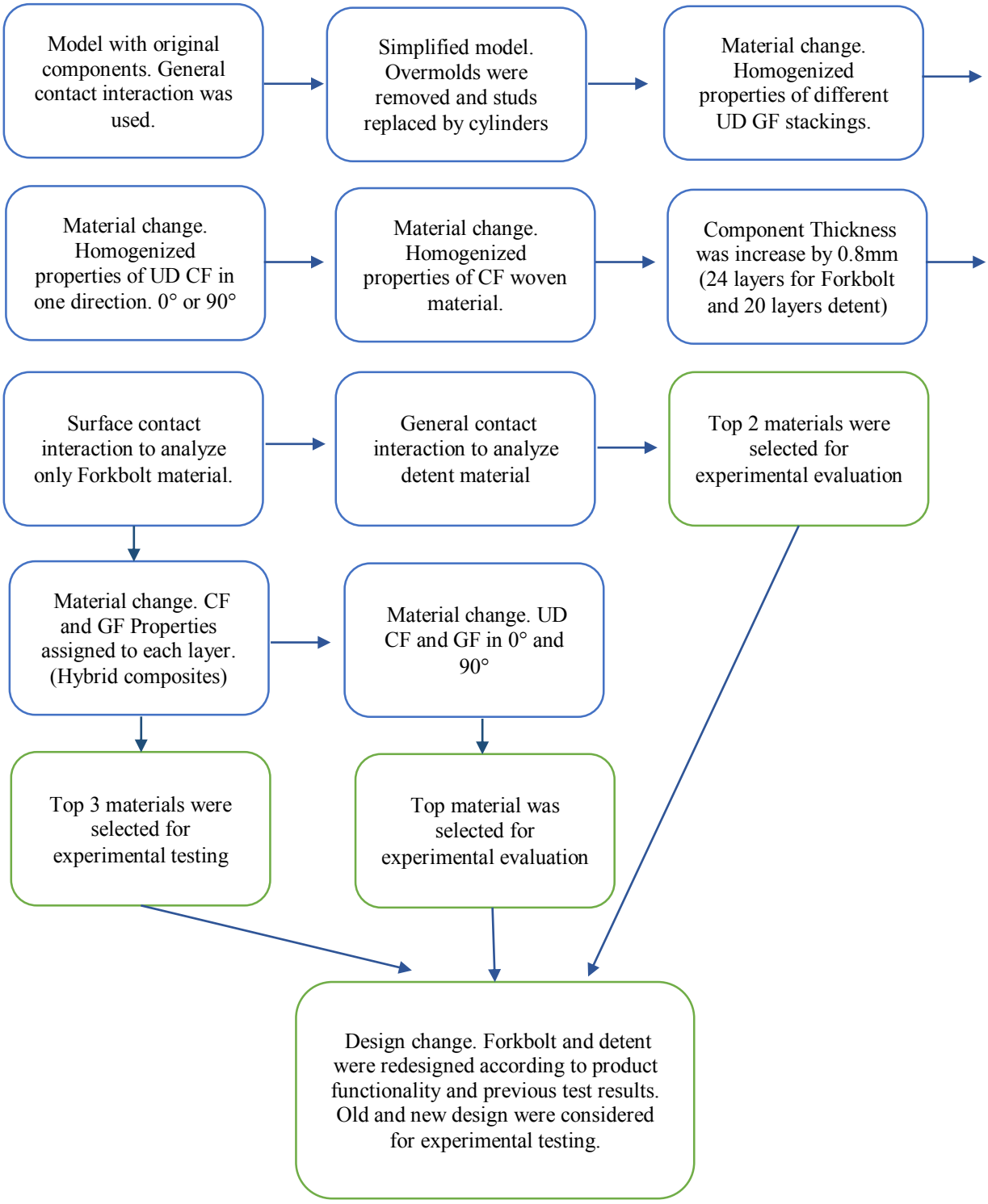

Figure 2.17: Computational Model Framework Flow Diagram

3. Experimental Procedure

3.1 Material System

Woven (plain wave) and unidirectional carbon fiber and glass fiber were used as reinforcement with EZ-Lam epoxy resin and hardener. Carbon and glass fiber woven fabrics, glass fiber unidirectional fabric and epoxy hardener kit were purchased from ACP Composites. Carbon fiber unidirectional fabric was purchased from fibreglast. Fiber fabric properties were given in Table 3.1. Epoxy resin and hardener were mixed at a weight ratio of 44:100 as it was recommended by manufacturer.

Table 3.1: Fabric Properties

Properties	Carbon Fabric	Glass Fabric	Carbon UD	Glass UD
Warp Material	3K Carbon Standard Modulus	S-Glass	12K Carbon Standard Modulus	407 tex S2 glass
Filling Material	3K Carbon Standard Modulus	S-Glass	-	-
Pattern	Plain Weave	Plain Weave	Unidirectional	Unidirectional
Weight	5.78 oz/yd^2	3.66 oz/yd^2	9 oz/yd^2	4 oz/yd^2
Thickness	.009 inches	.020 inches	0.014 inches	.009 inches

3.2 Manufacturing Process

Composite testing samples were manufactured by first building composite laminates using Vacuum Assisted Resin Transfer Molding (VARTM). VARTM is an advanced composite fabrication process and very effective to manufacture fiber-reinforced polymer composites. Normally, it is implemented when a large scale composite samples are needed. In other words,

several samples are manufacture at the same time by using VARTM. The VARTM manufacturing process goes as follows:

Firstly, fabrics needed to be cut to the desired laminate dimensions. All fabrics needed to build the laminate were stack up and placed between two metal plates along with nylon release peel ply, flow media ply and breathers as shown in Figure 3.1. The two aluminum plates function as molds and they were stick together by thermal tape placed on two opposite sides of the complete mold. Then, a spiral wrap tubing was placed to the sides, where there was no tape, to ensure the resin was spread uniformly throughout the mold. Next, the complete mold was enclosed in a vacuum bag as shown in Figure 3.2 (a) and impregnated with resin that went into the mold by an inlet port connected to one spiral wrap tube and then transferred into the fabrics by pressure gradient induced by vacuum pressure. Vacuum pressure was generated by a hydraulic pump, especially design for VARTM, connected to the other spiral wrap tubing which was the resin outlet when the fabrics were completely impregnated. Resin-hardener mix was debulked under vacuum before the resin impregnation process to avoid any air bubbles in the mix. Finally, when fibers were fully impregnated, the laminate was left to rest at room temperature for 24 hours to let the resin cure.

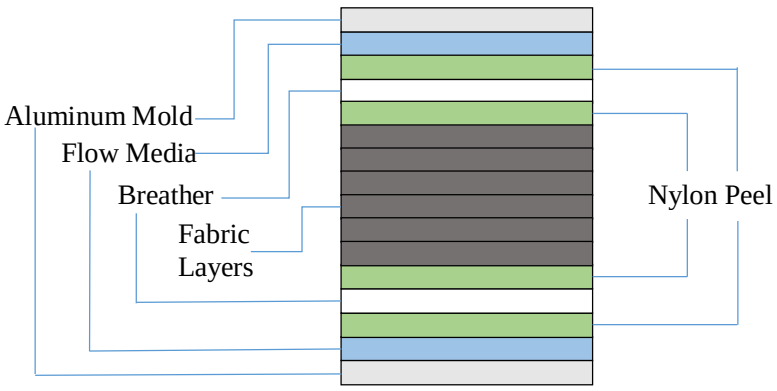

Figure 3.1: VARTM Material Layup

Finally, when the composite laminates completed their curing time, they were cut into the desired geometry by water jet cutting. During the waterjet cutting it was observed, that the CF24 unidirectional laminate was not fully impregnated of epoxy resin. Outer layers were solid and the fibers seemed to be fully impregnated. However, the inner layers were not solidified as seen in Figure 3.3 (a). Therefore, it was not possible to include unidirectional carbon fiber forkbolts in the experimental test. Moreover, it was observed on the cross section area of cut samples that there were cracks created by air trapped inside the laminate as seen in Figure 3.3 (b).

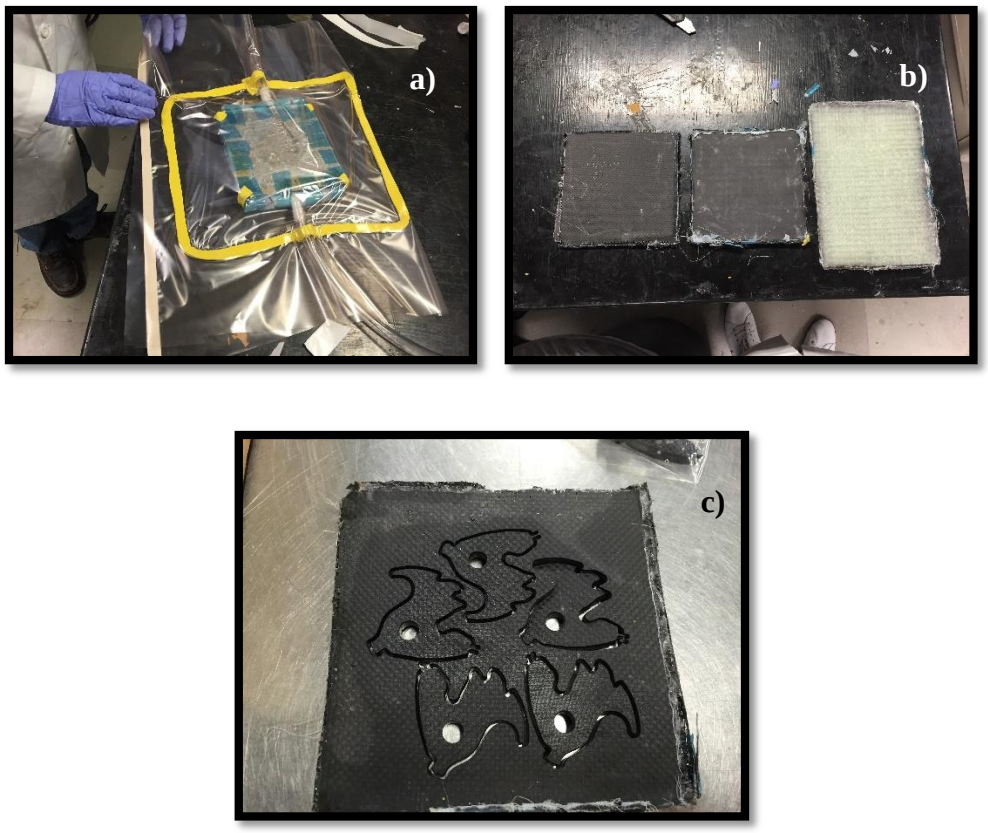

Figure 3.2: Manufacturing Process: (a) VARTM Mold Inside of Vacuum Bag; (b) Composite Laminates After 24 Hours of Curing; (c) Forkbolts Cut by Water Jet Cutting

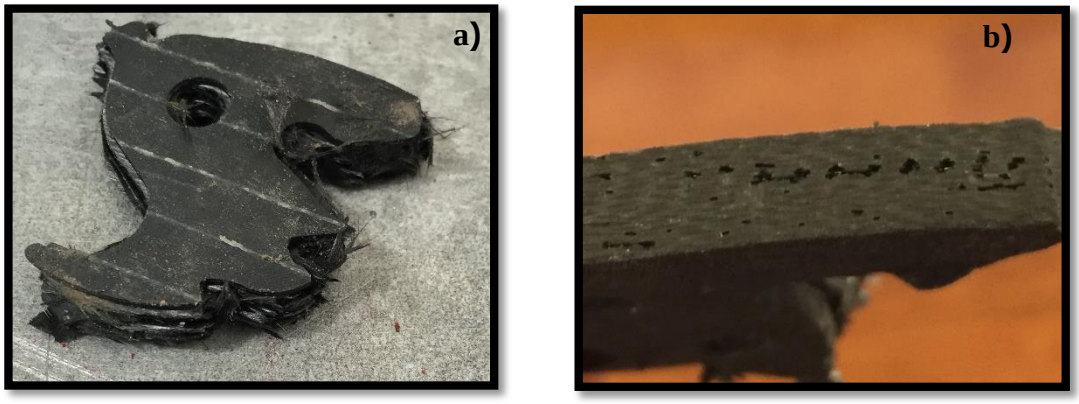

Figure 3.3: Observations After Water Jet Cutting: (a) Unidirectional CF24; (b) Cross-section of Woven CF24

3.4 TEST SETUP

A test setup was especially developed to only test forkbolt and detent instead of test the whole door latch system as it was done in the computational model. For this reason, a testing fixture was designed according to computational model boundary conditions. Testing fixture is shown in Figure 3.4. Forkbolt and detent were placed in their pins and pins went inside the main steel plate. Another plate was placed in the other end of the pins enclosing the components. Therefore, pins were not allowed to move in any direction. Fixture was fixed to the table as seen in Figure 3.4. Forkbolt was pulled up by the striker which was moved by the tensile testing machine. Tensile testing machine was setup to move up at a rate of 3.0 mm/min until the force cell reached a reading of above 6000 N or a significant force drop.

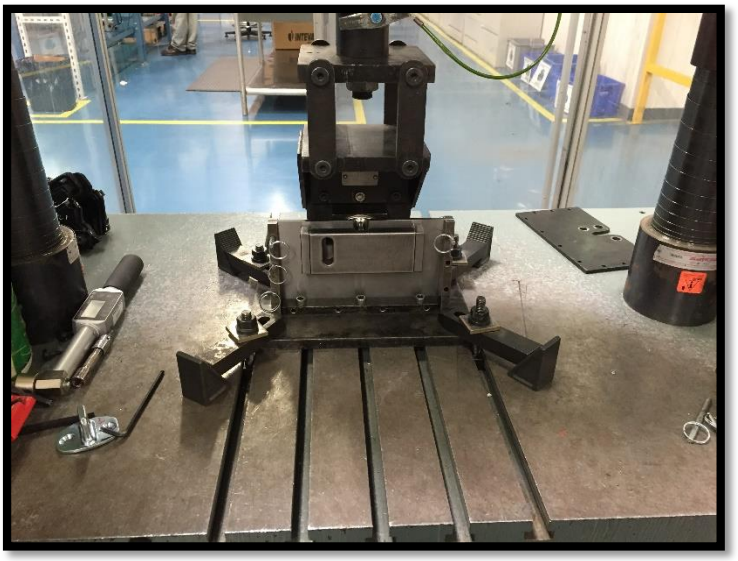

Figure 3.4: Testing Fixture

3.4 TESTING SAMPLES COMBINATIONS

Testing samples were chosen according to the computational model simulations. It was considered to test as many sample combinations in forkbolt and detent as possible in order to cross-relate results and validate conclusions done during the computational model. Also, it was contemplated to test the two forkbolt and detent designs studied before to compare both geometry results. All testing samples are shown in Table 3.2

3.5 TEST RESULTS

Fiber-reinforced composite forkbolt and detent were analyzed by exposing them to a simplified FMVSS No.206 transverse test. As a result, the tensile testing machine provided the load-displacement curve for all samples. The initial samples tested were three original design

100% woven carbon fiber forkbolts paired with three original design 100% woven glass fiber detents. Load-displacement curves for testing.

Sample combination 1 are shown in Figure3.5 (a). It was observed that the three samples did not reach the desired load of 5000 N. The maximum load reached for these samples was 3240 N and their average was 2850 N. Then, the next samples tested were three new design 100% woven carbon fiber forkbolts paired with three new design 100% woven glass fiber detents. Testing sample combination 2 results are shown in Figure 3.5 (b). By comparing the results from the first test and the second test it was noticed that the new design forkbolt and detent reached higher loads than the original design samples. The maximum load reached by the testing sample combination 2 was 4310 N and their average was 4030 N. Also, the load-displacement curves for these samples were very similar demonstrating the same behavior when the load was applied. Therefore, based on results, the new design of forkbolt and detent was stiffer than the original design. The same behavior was observed between both designs on the computational model results.

Subsequently, the following tests consisted of carbon-glass hybrid composite forkbolt coupled with woven and unidirectional glass fiber detent. The first testing sample combination tested was two samples of new design 75% woven carbon fiber and 25% woven glass fiber (CF9GF6CF9) forkbolts paired with two new design 100% woven glass fiber detents. Their load-displacement curves are shown in Figure 3.6 (a). It can be observed that one sample reached a load of 3980 N which was very close to the average load reached by the new design 100% carbon fiber forkbolt. However, there was a difference of 600 N between the average load of testing sample combination 2 and 3. Therefore, the 100% carbon fiber forkbolts were 15% stiffer than the 75%CF/25%GF. Then, the same hybrid forkbolt was tested but this time it was coupled with a new design 100% unidirectional glass fiber detent. The load-displacement curves for Testing sample

combination 4 are shown in Figure 3.6 (b). As a result, the maximum load reached was 2190 N and an the test average load was 2110 N. Unidirectional glass fiber detents did not performed as well as the woven glass fiber. In fact, the forkbolt-detent stiffness dropped by 38% when a unidirectional glass fiber detent was used instead of a woven glass fiber. Hence, the testing sample combination 4 recorded the lowest average loads in this study. Next, two new design 66.6% woven carbon fiber and 33.3% woven glass fiber (CF6GF12CF6) forkbolts were tested with two new design 100% woven glass fiber detents. Testing results were not accurate as it can be seen in Figure 3.6 (c). One sample reached a maximum load of 4210 N while the other sample reached a maximum load of 3100 N averaging a peak load of 3660 N. Even though the amount of samples was limited, it was observed that the 66.6%CF/33.3%GF forkbolt recorded higher loads than the 75%CF/25%GF forkbolt. Therefore, decreasing the carbon fiber percentage from 75% to 66.6% do not significantly impact the forkbolt stiffness. Finally, two new design 66.6% woven carbon fiber and 33.3% woven glass fiber forkbolts, like the ones tested in the previous test, were tested with two 100% unidirectional glass fiber detents. Their load-displacement curves are shown in in Figure 3.6 (d). The maximum load reached by one sample was 3510 N. Once again, the unidirectional glass fiber detents displayed lower maximum loads that the woven glass fiber detents by showing a test average of 3290 N. This test maximum load average was 10% lower than the testing combination 5. Also, the 66.6%CF/33.3%GF forkbolt recorded significant higher loads than the 75%CF/25%GF forkbolt when paired with a unidirectional glass fiber detent. In fact, the forkbolt-detent stiffness dropped by 35.86% when a unidirectional glass fiber detent was used instead of a woven glass fiber.

Table 3.2: Testing Sample Combinations

Testing Sample Combination	Forkbolt				Detent			
	Samples	Design	Fabric Type	Fiber Percentage	Samples	Design	Fabric Type	Fiber Percentage
1	3	Original	Woven	100% CF	3	Original	woven	100%GF
2	3	New	Woven	100% CF	3	New	woven	100%GF
3	2	New	Woven	75% CF 25% GF	2	New	woven	100%GF
4	2	New	Woven	75% CF 25% GF	2	New	UD	100%GF
5	2	New	Woven	66.6% CF 33.3% GF	3	New	Woven	100%GF
6	2	New	Woven	66.6% CF 33.3% GF	3	New	UD	100%GF

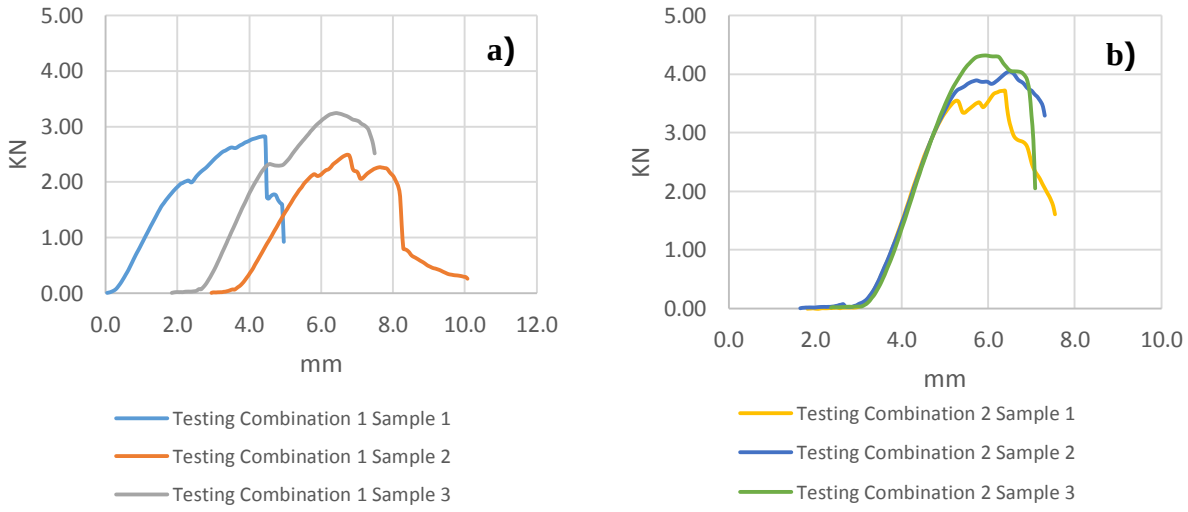

Figure 3.5: Testing Results of (a) Testing Combination 1 and (b) Testing Combination 2

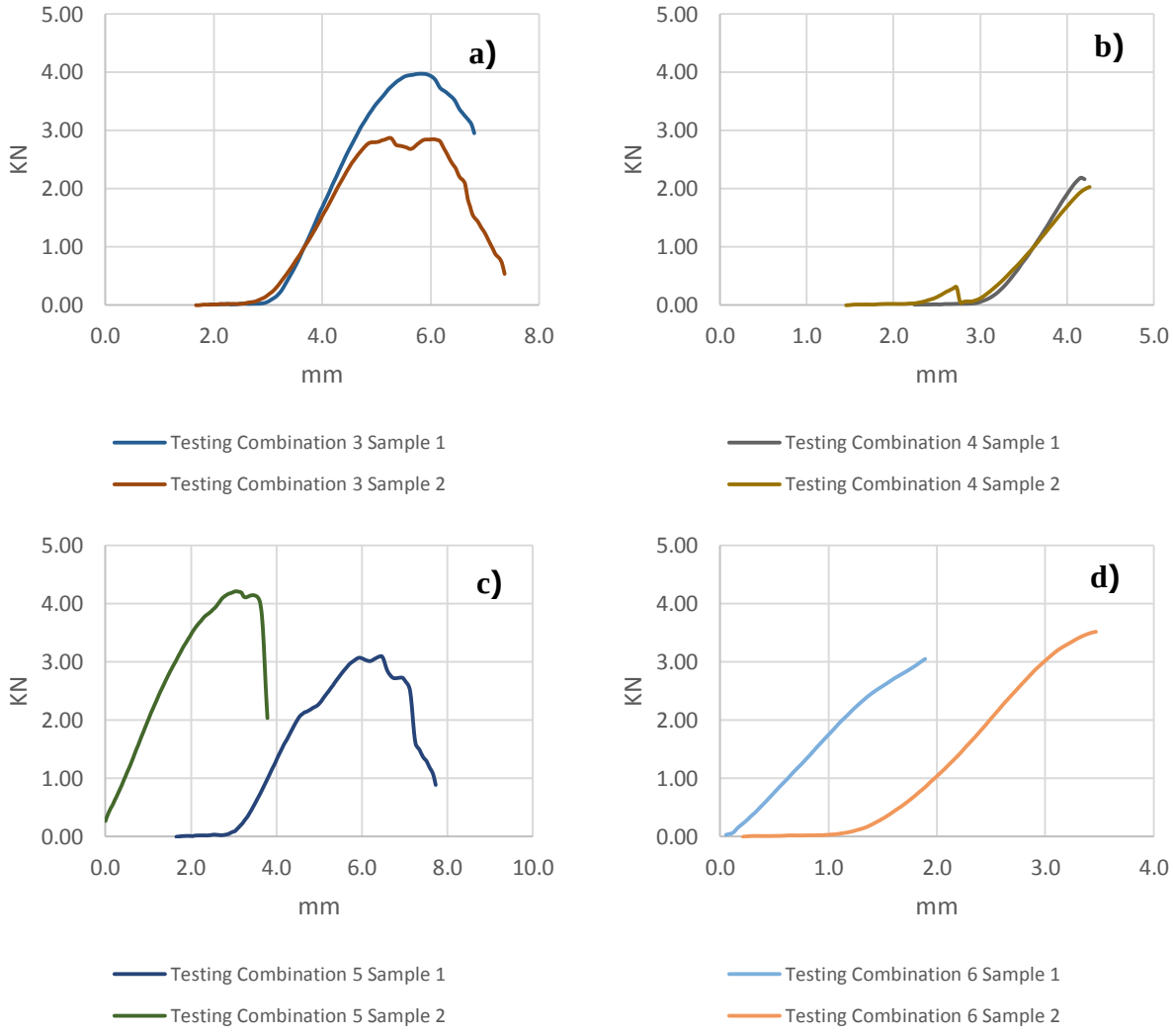

Figure 3.6: Testing Results of (a) Testing Combination 3, (b) Testing Combination 4, (c) Testing Combination 5 and (d) Testing Combination 6

3.7 DESIGN REVIEW BASED ON TEST RESULTS (DRBTR)

The DRBTR is a practical tool used in the automotive industry to evaluate the product design looking for buds of problems that are about to happen and/or potential defects on parts. DRBTR was conducted as part of this study to check the tested parts and examine component weaknesses. For this specific study, the failure was considered to be when the forkbolt was released by the detent. Therefore, the failure mode was what causes the forkbolt to be released. All testing samples were analyzed individually as follows:

Table 3.3: DRBTR

Testing sample combination	Sample	Analysis		Failure mode
		Forkbolt	Detent	
1	1	 Complete destruction of contact area with detent. Composite delamination.	 Slight deformation of contact area with forkbolt. Minor delamination.	Forkbolt area in contact with detent failed when load was applied letting the detent to slide out of contact.
	2	 Complete destruction of contact area with detent. Extensive composite delamination and cracking.	 Slight deformation of contact area with forkbolt. Minor delamination.	Forkbolt area in contact with detent failed when load was applied letting the detent to slide out of contact.

	3	 Complete destruction of contact area with detent. Detent penetration marks are visible. Minor delamination on contact.	 Slight deformation of contact area with forkbolt. A crack was formed one millimeter below contact.	Forkbolt area in contact with detent failed when load was applied letting the detent to penetrate and finally slide out of contact.
2	1	 Complete deformation of contact area with detent. No delamination or cracking.	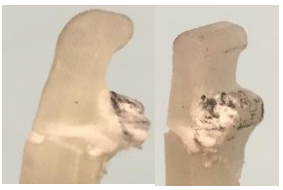 Complete destruction of detent head. Cracking all round detent head. Destruction of contact area with forkbolt.	Forkbolt and detent contact areas failed when load was applied. Components slided out of contact.
	2	 Complete deformation of contact area. minor delamination in contact.	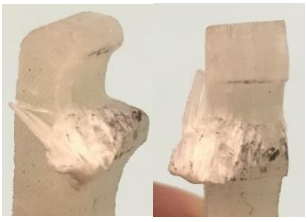 Complete destruction or contact area. Forkbolt penetration marks visible.	Forkbolt and detent contact areas failed when load was applied. Components slided out of contact.
	3	 Complete deformation of contact area. Minor delamination in contact.	 Complete destruction or contact area. Forkbolt penetration marks visible.	Forkbolt and detent contact areas failed when load was applied. Components slided out of contact.

3	1	 Complete deformation of contact area. minor delamination in contact and penetration marks.	 Complete destruction or contact area. Minor delamination on contact.	Forkbolt and detent contact areas failed when load was applied. Components penetrate each other until they slided out of contact.
	2	  Complete deformation of contact area. minor delamination in contact and penetration marks.	 Complete destruction or contact area. Minor delamination on contact.	Forkbolt and detent contact areas failed when load was applied. Components penetrate each other until they slided out of contact.
4	1	 Minimum wear on contact area.	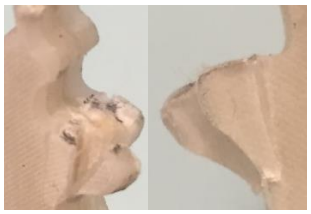 Complete destruction of contact area, significant delamination and cracking on contact.	Detent contact area failed when load was applied. Forkbolt penetrated and damaged detent until it was released.
	2	 Minimum wear on contact area.	 Complete destruction of detent head. Extensive cracking starting in contact area and delamination.	Detent contact area failed when load was applied. Forkbolt penetrated and damaged detent until it was released.

5	1	 Complete deformation of contact area. Delamination on contact.	 Complete destruction or contact area. Minor delamination on contact.	Forkbolt and detent contact areas failed when load was applied. Forkbolt was deformed in a sliding pattern. Detent was damaged liberating forkbolt.
	2	 Complete deformation of contact area. Delamination on contact.	 Complete destruction or contact area. Minor delamination on contact.	Forkbolt and detent contact areas failed when load was applied. Forkbolt was deformed in a sliding pattern. Detent was damaged liberating forkbolt.
6	1	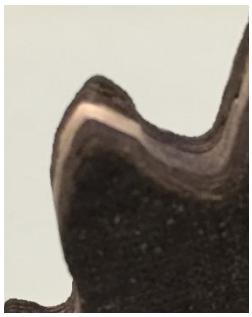 Minimum penetration mark on contact. No delamination.	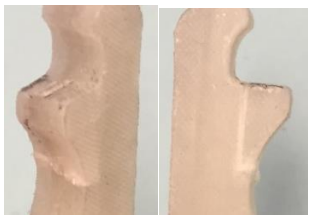 Cracking starting in contact and continued below detent head. No delamination.	Forkbolt contact area and Detent failed. Components slided out of contact.
	2	 Minimum penetration mark on contact. Contact area turned. No delamination.	 Cracking starting in contact and continued below detent head. No delamination.	Forkbolt contact area and Detent failed. Components slided out of contact.

3.7 CONCLUDING REMARKS

Fiber-reinforced composite forkbolt and detent were analyzed in this study by exposing them to a simplified FMVSS No.206 transverse test. A computational model was utilized to iterate the material properties and approximate testing results. Also, an experimental procedure was performed according to the computational model to validate results. Six sample combinations were studied including forkbolts made of woven 100%CF, 75%CF/25%GF, 66.6%CF/33.3%GF and detents made of woven 100%GF and unidirectional 100%GF. Computational model and experiment results revealed that substituting few layers of carbon fiber with glass fiber do not significantly impact the forkbolt stiffness. For instance, test results recorded a stiffness drop of 15% when the carbon fiber percentage decreases from 100% to 75%. A similar pattern in shown in the computational model where stiffness drop is 10%. Also, it was observed in the experimental testing that woven glass fiber detent was superior to the unidirectional glass fiber detent by presenting a forkbolt-detent stiffness 38% higher. In fact, the computational model concluded that woven fiber-reinforced composite components were stiffer than the unidirectional fiber-reinforced composite components. Moreover, the current and new design of forkbolt and detent were studied. While the computational model noted a stiffness increment of 24% after the components were redesigned, experimental testing showed a stiffness increment of 29%.

Furthermore, it was observed in the experimental procedure results that fiber-reinforced composite forkbolt and detent did not reach the desired load of 5000 N. However, the redesigned forkbolt made of 100% woven carbon fiber and the redesigned detent made of 100% woven glass fiber were close to reach that load. The design review based on test results performed (DRBTR) showed that components did not fail where the computational model concluded to be the areas with the highest maximum principal stress. In contrast to the computational model, all samples

failed at the contact area between forkbolt and detent. Computational model and experimental testing results differed from each other because in the computational model homogenized material properties were assigned to each layer. In other words, the computational model did not distinguish from fiber and matrix mechanical properties. Moreover, result differed because the cross-section material hardness properties were not considered in this study. Consequently, future studies in the implementation of fiber-reinforced composite materials into a door latch system must study the cross-section material hardness.

References

[1] U.S. Department of Transportation. Laboratory test procedure for FMVSS No. 206 door locks and door retention components. Federal Motor Vehicle Safety Standards, 2010.

[2] A.R. Abu Talib, Aidy Ali, Mohamed A. Badie, Nur Azida Che Lah, A.F. Golestaneh. Developing a hybrid, carbon/glass fiber-reinforced, epoxy composite automotive drive shaft. Materials and Design, 31(1):514-521, 2010.

[3] Jin Zhang, Khunlavit Chaisombat, Shuai He, Chun H. Wang. Hybrid composite laminates reinforced with glass/carbon woven fabrics for lightweight load bearing structures. Materials and Design, 36:75-80, 2012.

[4] Al-Qureshi HA. Automobile leaf springs from composite materials. Journal of Materials Processing Technology, 118:58-61, 2001.

[5] Hosseinzadeh R, Shkreih MM, Lessard LB. Parametric study of automotive composite bumper beams subjected to low-velocity impacts. Composite Structures, 68:419-427, 2005.

[6] Kedar S. Pandya, Ch. Veerraju, N.K. Naik. Hybrid composites made of carbon and glass woven fabrics under quasi-static loading. Materials and Design. 32(7):4094-4099, 2011.

[7] Cramer DR, Taggart DF. Design and manufacture of an affordable advanced-composite automotive body structure. In: The 19th international battery, hybrid and fuel cell electric vehicle symposium & exhibition, 2002.

[8] Beardmore P, Johnson CF. The potential for composites in structural automotive applications. Composite Science and Technology, 26:251-281, 1986.

[9] Das S. The cost of automotive polymer composites: a review and assessment of DOE's lightweight materials composites research. Oak Ridge Natural Laboratory, 2001.

[10] Bunsell AR, Harris B. Hybrid carbon and glass fibre composites. Composites, 5:157-164. 1974.

[11] Chensong Dong, Ian J. Davies. Optimal design for the flexural behavior of glass and carbon fibre reinforced polymer hybrid composites. Materials and Design, 37:450-457, 2012.

[12] R.M. Christensen and F.M. Waals. Effective stiffness of randomly oriented fibre composites. Journal of Composite Materials 6(3):518-535, 1972.

Appendix

A.1 Computational Model Investigation

The first challenge encountered in this study was to efficiently simulate a door latch system according to the strength test FMVSS No. 206 by using a computational model. A door latch system is an assembly with more than twenty components. Therefore, creating a computational model that includes all of the components is very laborious and time-consuming. A computational model investigation was performed in order to find the most accurate and time-efficient model. Firstly, it was investigated the components that have the most impact on strength test and the ones that have the least impact to it. The latch system was analyzed as a structure and all plastic components that are not part of the structure were not considered to be part of the computational model. Consequently, the only components that are part of the latch system structure are the forkbolt subassembly (core and overmold), detent subassembly (core and overmold), forkbolt stud, detent stud, steel frame and reinforcement plate. However, steel frame and reinforcement were not considered to be part of the computational model. Thereupon, the computational model was developed progressively starting with the forkbolt subassembly. Then, the remaining components were included to the model.

The first model consisted of only the forkbolt subassembly was developed by merging the whole subassembly into one component. Component boundaries and material properties of both components were preserved. The forkbolt overmold cylindrical face that rotates around the stud was fixed in all directions. The forkbolt face that is originally in contact with detent is also fixed as part of the model boundary conditions. Moreover, a representative force is applied to the forkbolt in the door closing direction. As a result, the model run successfully concluding that the

forkbolt subassembly can be merged into one component. Then, the second computational model consisted of the forkbolt subassembly, forkbolt stud, detent subassembly and detent stud. The same approach used in the previous simulation was utilized. So, the forkbolt and detent subassemblies were merged into two components. However, a constraint needs to be added to the interaction between studs and subassemblies. Also, the contact between forkbolt and detent must be evaluated. Consequently, it was decided to divide the model into two parts by merging subassemblies with their corresponding studs. Furthermore, a general contact condition was assigned to the whole model throughout the time steps. Also, both studs were fixed in all directions at their ends where they originally interact to the rest of the latch structure and a force of 9000N was applied as specified in FMVSS No. 206. As a result, the computational model run successfully showing a satisfactory contact behavior between the two merged components studied. However, Maximum principal stresses shown in results are extremely high (Figure A.1 shows the maximum principal stress contours). Therefore, it is concluded that a lower force needs to be applied to the model since the force specified in FMVSS No. 206 applies to the whole latch system structure.

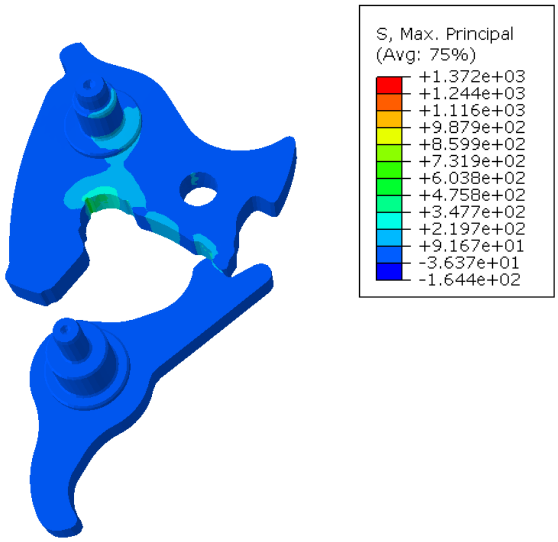

Figure A.1: Maximum Principal Stress Contours of Original Design Model

It was observed on the previous model that stud and forkbolt elements were twisted on the results deformed view due to the boundary conditions defined on the model. Since twisted elements may show different stress behavior than in reality, new contact conditions were studied in the same components. The objective of the following model was to successfully employ a contact condition between components and their studs; especially, on the interaction between forkbolt and stud where forkbolt elements in contact with stud should rotate around stud instead of twisting with it. For this reason, forkbolt and detent subassemblies were unmerged from studs in the model. The first contact condition studied was surface to surface contact in the whole model. Therefore, surfaces in contact needed to be individually selected. Stud faces in contact with forkbolt and detent were selected as the master surface, and forkbolt and detent faces in contact with studs were selected as the slave surfaces. Also, the forkbolt surface in contact with detent was selected as the master surface and the detent surface in contact with detent was selected as the master surface. As a result, the computational model could not be solved by the software giving several errors. Then, the same model was developed with modifications on the contact condition. The same contact condition was selected than in the previous model but master and slave surfaces were swapped. For example, the stud surfaces were selected as slave surface and the forkbolt and detent surfaces in contact with studs were selected as master surfaces. Unfortunately, the changes in the surface to surface contact did not change the previous unsuccessful results. Furthermore, more iterations were done to the model to define the contact between elements. For instance, it was tried to apply constraints to the parts instead of interactions but the results did not variate. Ultimately, a new model was constructed in which only forkbolt subassembly and its stud was studied. The intention of removing components from the model was to exclusively analyze the contact between forkbolt subassembly and its stud. The surface to surface contact interactions was

chosen one again. The forkbolt surface in contact with stud was selected as the slave surface and the stud surface in contact with forkbolt was selected as the master surface. Moreover, the forkbolt face originally in contact with detent was fixed in all directions as it was done in the first model studied. As a result, the model was solved successfully. It was observed in the results deformed view that forkbolt elements in contact with detent appropriately rotated around detent as seen in Figure A.2. Consequently, the surface to surface contact interaction can successfully be implemented to exclusively analyze forkbolt subassembly and its stud. However, results on this computational model study showed that its implementation on a forkbolt and detent analysis is not feasible.

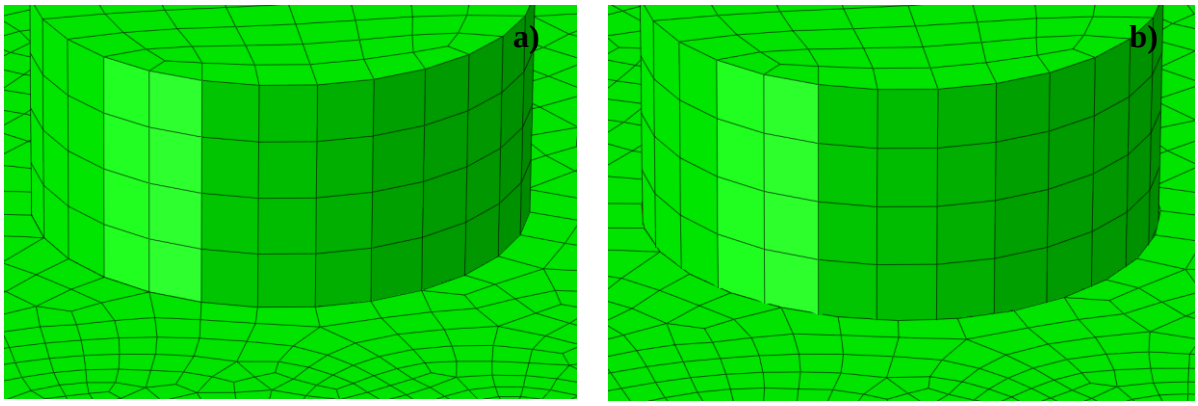

Figure A.2: Forkbolt Rotation around Stud (a) before and (a) after

As has been noted, only two computational models were accurately solved. One computational model employs a general contact interaction to analyze forkbolt and detent subassemblies with its studs. On the other hand, the other computational model employs a surface to surface contact interaction to only evaluate forkbolt subassembly and its stud. It was observed that both approaches showed similar results on forkbolt by comparing the forkbolt maximum principal stresses. However, the surface contact approach provided superior stress distribution contours than the general contact approach. Consequently, the surface contact approach can be

used to analyze forkbolt in further studies and the general contact approach can be utilized to study contact pressures in forkbolt-detent contact and detent maximum principal stresses.

A.2 COMPOSITE CYLINDER MODEL (CCM)

In the CCM it is assumed that the volume of the composite is completely filled with cylindrical fibers and each of them is surrounded by a cylinder filled by matrix material. Also, it is assumed that each of the fiber-matrix concentric cylinders has the same fiber volume fraction a she entire composite. CCM effectively represents a lamina within a laminate and behaves as a transversely isotropic material. Unfortunately, CCM only provides four of the five elastic constants. So, G_{23} is calculated with the Generalized Self Consistent Scheme (GSCS) in conjunction with CCM

The following CCM equations [12] are used to determine the axial homogenized elastic properties of the lamina. "1" represents the fiber direction, the subscript "f" denotes fiber and subscript "m" denotes matrix.

Axial modulus:

$$E_1 = E_1^f(1+\gamma)V^f + E^m(1+\delta)(1-V^f)$$

Where,

$$\gamma = \frac{2v_{21}^f E^m\left(1 - v_{23}^f - 2v_{12}^f v_{21}^f\right)V^f\left(v_{12}^f - v^m\right)}{E_2^f(1+v^m)\left(1+V^f(1-2v^m)\right) + E_m\left(1 - v_{23}^f - 2v_{12}^f v_{21}^f\right)(1-V^f)}$$

$$\delta = \frac{2E_2^f v^m V^f\left(v^m - v_{12}^f\right)}{E_2^f(1+v^m)\left(1+V^f(1-2v^m)\right) + E_m\left(1 - v_{23}^f - 2v_{12}^f v_{21}^f\right)(1-V^f)}$$

Transverse modulus:

$$E_2 = \frac{1}{\frac{\eta^f V^f}{E_2^f} + \frac{\eta^m (1 - V^f)}{E^m}}$$

$$E_3 = E_2$$

Where,

$$n^f = \frac{E_1^f V^f + \left[\left(1 - v_{12}^f v_{21}^f\right) E^m + v^m v_{21}^f E_1^f\right](1 - v^f)}{E_1^f V^f + E^m (1 - V^f)}$$

$$n^m = \frac{\left[\left(1 - v^{m^2}\right) E_1^f - \left(1 - v^m v_{12}^f\right) E^m\right] V^f + E^m V^m}{E_1^f V^f + E^m (1 - V^f)}$$

Axial Poisson's ratio:

$$v_{12} = \frac{\left[(1 - V^f)\left(1 - v_{23}^f - 2 v_{12}^f v_{21}^f\right)\right] v^m E^m}{\left((1 - V^f)\left(1 - v_{23}^f - 2 v_{12}^f v_{21}^f\right)\right) E^m + \left(1 + V^f + (1 - V^f) v^m - 2 V^f v^{m^2}\right) E_2^f}$$

$$+ \frac{\left[v^m + V^f\left(2 v_{12}^f - v^m\right) + \left(v^{m^2}\left(1 - 2 V^f v_{12}^f - V^f\right)\right)\right] E_2^f}{\left((1 - V^f)\left(1 - v_{23}^f - 2 v_{12}^f v_{21}^f\right)\right) E^m + \left(1 + V^f + (1 - V^f) v^m - 2 V^f v^{m^2}\right) E_2^f}$$

Axial Shear Modulus:

$$\mu_{12} = G_{12} = G^m \left[\frac{\left(G^m + G_{12}^f\right) - V^f\left(G^m - G_{12}^f\right)}{\left(G^m + G_{12}^f\right) - V^f\left(G^m - G_{12}^f\right)}\right]$$

Transverse Shear Modulus:

$$G_{23}^* = \frac{\frac{1}{\frac{1}{G_{23}^f} V^f + \eta_4 \frac{1}{G^m} (1 - V^f)}}{V^f + \eta_4 (1 - V^f)}$$

Where,

$$\eta_4 = \frac{3 - 4 v^m + \frac{G^m}{G_{23}^f}}{4(1 - v^m)}$$

A.3 CLASSICAL LAMINATION THEORY (CLT)

The CLT is utilized to determine the mechanical properties of a laminated composite. This theory analyzes a composite built by many laminas in which each lamina consists of unidirectional fibers and matrix. The fibers in each lamina can be oriented differently than the fibers in the other laminas. For example, Talib et al. employed this theory to analyze the material properties of a drive shaft which is built by carbon and glass unidirectional fiber laminas oriented in various directions []. The CLT starts by calculating a reduced stiffness matrix for each lamina considering the fiber angle. Then, the reduced stiffness coefficients of all laminas are integrated to create a notion of stress resultants and moment resultants. Therefore, this integration gives a thickness average stiffness matrix called ABBD matrix shown in () and (). The ABBD matrix is a homogenized stiffness matrix of the entire laminated composite and. A, B and D coefficients are calculated as:

$$A_{ij} = \sum_{k=1}^{n} \left(\bar{Q}_{ij}\right)_k (h_k - h_{k-1})$$

$$B_{ij} = \frac{1}{2} \sum_{k=1}^{n} \left(\bar{Q}_{ij}\right)_k (h_k^2 - h_{k-1}^2)$$

$$D_{ij} = \frac{1}{3} \sum_{k=1}^{n} \left(\bar{Q}_{ij}\right)_k (h_k^3 - h_{k-1}^3)$$

$$\begin{Bmatrix} N_x \\ N_y \\ N_{xy} \end{Bmatrix} = \begin{bmatrix} A_{11} & A_{12} & A_{16} \\ A_{12} & A_{22} & A_{26} \\ A_{16} & A_{26} & A_{66} \end{bmatrix} \begin{Bmatrix} \epsilon_x^0 \\ \epsilon_y^0 \\ \gamma_{xy}^0 \end{Bmatrix} + \begin{bmatrix} B_{11} & B_{12} & B_{16} \\ B_{12} & B_{22} & B_{26} \\ B_{16} & B_{26} & B_{66} \end{bmatrix} \begin{Bmatrix} \chi_x \\ \chi_y \\ \chi_{xy} \end{Bmatrix}$$

$$\begin{Bmatrix} M_x \\ M_y \\ M_{xy} \end{Bmatrix} = \begin{bmatrix} B_{11} & B_{12} & B_{16} \\ B_{12} & B_{22} & B_{26} \\ B_{16} & B_{26} & B_{66} \end{bmatrix} \begin{Bmatrix} \epsilon_x^0 \\ \epsilon_y^0 \\ \gamma_{xy}^0 \end{Bmatrix} + \begin{bmatrix} D_{11} & D_{12} & D_{16} \\ D_{12} & D_{22} & D_{26} \\ D_{16} & D_{26} & D_{66} \end{bmatrix} \begin{Bmatrix} \chi_x \\ \chi_y \\ \chi_{xy} \end{Bmatrix}$$

Vita

Francisco Javier Guevara Arreola has 25 years old and he was born in Chihuahua, Mexico. He moved to El Paso, Texas to enroll at The University of Texas at El Paso where he was awarded with a bachelor's degree in Mechanical Engineering in fall of 2013 at the University of Texas at El Paso. Then, in spring 2014, He entered to the Graduate School at The University of Texas pursuing a Master's degree in Mechanical Engineering. After the first semester he got hired by a tier-1 automotive supplier in Juarez, Mexico where he has worked as a product engineer. While being a full time engineer, he started researching about the implementation of carbon, glass and carbon-glass hybrid composite materials into a door latch system. After two years in Graduate School, He earned a Master's degree in Mechanical Engineering.

Permanent address: Gabriela Mistral 2515

Chihuahua, Mexico 31130

Francisco Javier Guevara Arreola